

AD-A041 380

CLARKSON COLL OF TECHNOLOGY POTSDAM N Y DEPT OF CIVI--ETC F/G 11/2
STRENGTH OF STEEL FIBER CONCRETE IN ADVERSE ENVIRONMENTS. (U)
JUN 77 G B BATSON

DACA88-75-C-0004

UNCLASSIFIED

CERL-SR-M-218

NL

6 OF 1

AD A041 380



				<p>END DATE FILMED 7-77</p>								

construction
engineering
research
laboratory

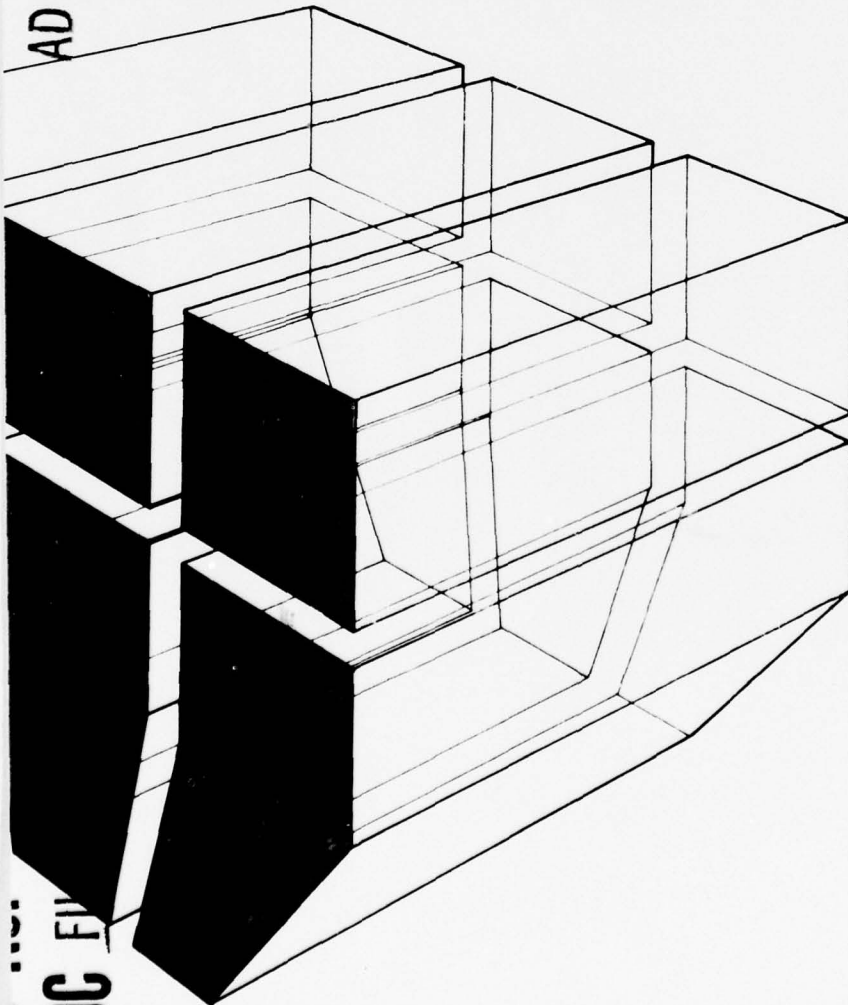
Handwritten initials

SPECIAL REPORT M-218
June 1977
Corrosion Behavior of Cracked Fibrous Concrete

ADA 041380

STRENGTH OF STEEL FIBER CONCRETE
IN ADVERSE ENVIRONMENTS

by
G. B. Batson



DDC FILE

DDC
RECORDS
JUL 6 1977
D



The contents of this report are not to be used for advertising, publication, or promotional purposes. Citation of trade names does not constitute an official indorsement or approval of the use of such commercial products. The findings of this report are not to be construed as an official Department of the Army position, unless so designated by other authorized documents.

*DESTROY THIS REPORT WHEN IT IS NO LONGER NEEDED
DO NOT RETURN IT TO THE ORIGINATOR*

19 REPORT DOCUMENTATION PAGE		READ INSTRUCTIONS BEFORE COMPLETING FORM
1. REPORT NUMBER 18 CERL-SR-M-218	2. GOVT ACCESSION NO.	3. RECIPIENT'S CATALOG NUMBER
4. TITLE (and Subtitle) 6 STRENGTH OF STEEL FIBER CONCRETE IN ADVERSE ENVIRONMENTS	5. TYPE OF REPORT & PERIOD COVERED 9 FINAL <i>repts</i>	
	6. PERFORMING ORG. REPORT NUMBER	
7. AUTHOR(s) 10 Gordon B. Batson	8. CONTRACT OR GRANT NUMBER(s) 15 DACA88-75-C-0004 <i>new</i>	
9. PERFORMING ORGANIZATION NAME AND ADDRESS CONSTRUCTION ENGINEERING RESEARCH LABORATORY P.O. Box 4005 Champaign, IL 61820	10. PROGRAM ELEMENT, PROJECT, TASK AREA & WORK UNIT NUMBERS 16 4A762719AT41-T7-003	
11. CONTROLLING OFFICE NAME AND ADDRESS <i>410264</i> Clarkson Coll. of Technology, Potsdam, NY Dept. of Civil and Environmental Engineering	12. REPORT DATE 17 June 1977 17 77	
14. MONITORING AGENCY NAME & ADDRESS (if different from Controlling Office) 12 57p.	13. NUMBER OF PAGES 35	
	15. SECURITY CLASS. (of this report) UNCLASSIFIED	
15a. DECLASSIFICATION/DOWNGRADING SCHEDULE		
16. DISTRIBUTION STATEMENT (of this Report) Approved for public release; distribution unlimited.		
17. DISTRIBUTION STATEMENT (of the abstract entered in Block 20, if different from Report)		
18. SUPPLEMENTARY NOTES Copies are obtainable from National Technical Information Service, Springfield, VA 22151		
19. KEY WORDS (Continue on reverse side if necessary and identify by block number) saltwater steel-fiber-reinforced concrete wedge opening loading specimen		
20. ABSTRACT (Continue on reverse side if necessary and identify by block number) This report presents the results of an investigation of the strength of cracked steel-fiber-reinforced concrete subjected to a flowing salt-water environment. The testing procedure was adapted from the plane strain fracture toughness method of testing metallic materials using a modified wedge opening loading (WOL) specimen.		

410 264

LB

BLOCK 20 (cont'd)

→ Concrete specimens were cast with 1.0, 1.5, and 2.0 percent concentrations of steel fibers by volume of concrete and cured for 28 days in a moisture room. After 28 days, a notch was sawed in each of the specimens with a masonry saw, and a small crack was propagated from the tip of the notch by mechanical means. Control specimens then underwent a compliance testing procedure to determine the work rate necessary to propagate a crack through the specimens. The remaining specimens were subjected to a flowing saltwater environment for four different exposure intervals. The strain energy release rate of the specimens exposed to saltwater was determined and compared with that of the control specimens. The rate of change of strain energy release rate decreased with increasing time and with increasing steel fiber content.

UNCLASSIFIED

FOREWORD

This study was conducted for the Directorate of Military Construction, Office of the Chief of Engineers (OCE) under Project 4A762719AT41, "Design, Construction, and Operations and Maintenance for Military Facilities"; Task T7, "Materials Research and Development for Military Construction"; Work Unit 003, "Corrosion Behavior of Cracked Fibrous Concrete." The applicable QCR number is 1.03.007. Mr. S. Gillespie was the OCE Technical Monitor.

The work was performed under Contract No. DACA 88-75-C-0004 by Dr. Gordon B. Batson, Civil and Environmental Engineering Department, Clarkson College of Technology, Potsdam, NY. Mr. John Obzsarski was a research assistant for the project. The work was performed for the Construction Materials Branch (MSC), Materials and Science Division (MS), U.S. Army Construction Engineering Research Laboratory (CERL), Champaign, IL.

Mr. P. Howdysshell is Chief of MSC, and Dr. G. Williamson is Chief of MS. COL J. E. Hays is Commander and Director of CERL, and Dr. L. R. Shaffer is Technical Director.

ACCESSION for	
NTIS	White Section <input checked="" type="checkbox"/>
DDC	Soft Section <input type="checkbox"/>
UNANNOUNCED	<input type="checkbox"/>
JUSTIFICATION.....	
BY	
DISTRIBUTION/AVAILABILITY CODES	
REF.	AVAIL. REP./SPECIAL
A	

DDC
RECORDED
JUL 8 1977
RECEIVED
D

CONTENTS

	DD FORM 1473	1
	FOREWORD	3
	LIST OF TABLES AND FIGURES	5
1	INTRODUCTION.	7
	Background	
	Purpose	
	Approach	
2	TESTING PROGRAM	11
	Test Specimen	
	Specimen Casting Procedure	
	Control Specimen Testing Procedure	
	Environmental Specimen Testing Procedure	
	Compliance Analysis	
3	RESULTS	23
4	DISCUSSION OF TEST RESULTS.	36
5	POTENTIAL STRUCTURAL APPLICATIONS	38
6	CONCLUSIONS AND RECOMMENDATIONS	40
	APPENDIX A: FRACTURE MECHANICS THEORY	41
	APPENDIX B: CURVE FIT DERIVATION AND COMPUTER PROGRAM	43
	REFERENCES	53
	DISTRIBUTION	

FIGURES

<u>Number</u>		<u>Page</u>
1	Modified WOL Specimen	9
2	Steel Fibers	12
3	Mechanical Cracking Harness	13
4	Electromechanical Testing Machine	14
5	Autographic Recorder	15
6	Compliance Gage	15
7	Schematic of Compliance Gage	16
8	Specimens Prepared for Testing	17
9	Typical Load-Displacement Relationship	18
10	Environmental Exposure Tank	19
11	Critical Strain Energy Release Rate for 1.0 Percent Fiber Content	25
12	Relative Critical Strain Energy Release Rates	26
13	Compliance Curve Fit for 1.0 Percent Fiber Content	30
14	Compliance Curve Fit for 1.5 Percent Fiber Content	30
15	Compliance Curve Fit for 2.0 Percent Fiber Content	31
16	Theoretical Compliance Curve and Compliance Curve Fit for 1.0, 1.5, and 2.0 Percent Fiber Content	34
17	Strength Analysis of a Crack Member in Bending	39

TABLES

1	Mix Design	11
2	Critical Strain Energy Release Rates of Environmental Specimens	23
3	Student 't' Test for Average G_{IC} Values	27
4	Compliance, Crack Onset, and Ultimate Loads of Control Specimens	29

TABLES (cont'd)

<u>Number</u>		<u>Page</u>
5	Critical Strain Energy Release Rate of Control Specimens	32
6	Compressive Strength Cylinders	33
7	Properties of Artificial Saltwater Environment	35

STRENGTH OF STEEL FIBER CONCRETE IN ADVERSE ENVIRONMENTS

1 INTRODUCTION

Background

Introduction of randomly dispersed discrete steel fibers into a concrete mix significantly alters the strength characteristics of the plain concrete. Of particular concern is the change in strength as cracks develop and propagate through fibrous concrete exposed to a flowing saltwater environment--conditions to which a fibrous concrete overlay of a pavement or bridge deck would be exposed.

This study investigated this problem using fracture mechanics. Fracture mechanics, which A. A. Griffith proposed as a theory explaining brittle failure in 1921,¹ involves use of energy relationships to determine a material's strength by relating inherent flaw dimensions to the material's state of stress. (Appendix A explains the theory in greater detail.) Fracture mechanics was initially applied to brittle materials such as glass, but was later modified by Irwin for application to ductile materials such as steel.² Interest in using fracture mechanics to explain the failure mechanism of both plain and fiber-reinforced concrete³ has been growing.

The introduction of randomly distributed discrete steel fibers directly into the concrete mix improves many of the important mechanical properties of plain concrete, such as the flexure, tensile, and fatigue strengths.⁴⁻⁶ The average spacing of fibers is less than 0.200 in.

¹A. A. Griffith, "Phenomena of Rupture and Flow in Solids," *Philosophical Transactions*, Vol 221, No. A587 (Royal Society of London, 1921), p 163.

²G. R. Irwin and J. A. Kies, "Critical Energy Rate Analysis of Fracture Strength," *Welding Journal*, Vol 33 (April 1954), p 193s.

³J. P. Romualdi and G. B. Batson, "Mechanics of Crack Arrest in Concrete," *Journal of the Engineering Mechanics Division, Proceedings of the American Society of Civil Engineers*, Vol 89, No. EM3 (June 1963), p 147.

⁴G. B. Batson, et al., "Flexural Fatigue of Steel Fiber Reinforced Concrete Beams," *Journal of the American Concrete Institute*, Proceedings Vol 69, No. 11 (November 1972), p 673.

⁵G. B. Batson, E. Jenkins, and R. Spatney, "Steel Fibers as Shear Reinforcement in Beams," *Journal of the American Concrete Institute*, Proceedings Vol 69, No. 10 (October 1972), p 640.

⁶R. N. Swamy and P. S. Mangat, "The Onset of Cracking and Ductility of Steel Fiber Reinforced Concrete," *Cement and Concrete Research*, Vol 5 (1975), p 37.

(5.08 mm) for concentration of steel fibers in the range of 1 or 2 percent.^{7,8} The close spacing of the fibers, which act as crack arrestors, inhibits or retards the growth of flaws existing naturally in the concrete. The crack-arrest action increases the first-crack strength (i.e., the point at which the load-deflection relationship is no longer linear), and greatly improves the ductility after cracking by consuming energy to pull out or strip steel fibers from the concrete matrix.⁹

Purpose

The purpose of this study was to determine the reduction in strength of steel-fiber-reinforced concrete when a sharp crack in the fiber concrete is subjected to an applied stress normal to the direction of the crack after exposure to continually flowing saltwater for varying durations of time.

Approach

The experimental technique employed is an adaptation of the plane strain fracture toughness testing technique.¹⁰ Wedge opening loading (WOL) specimens, which have been widely used for experimental verification of theoretical fracture phenomena,¹¹ were used. The main advantages of the WOL specimen are its compactness and convenience for laboratory machining and testing. A scaled-up WOL specimen (Figure 1) has been employed for previous fiber concrete research.^{12,13} The dimensions of the specimen are such that a significant volume of the material has a random distribution of fibers; only near the surfaces is there any preferential alignment.

⁷Swamy and Mangat.

⁸J. P. Romualdi and J. A. Mandel, "Tensile Strength of Concrete Affected by Uniformly Distributed and Closely Spaced Short Lengths of Wire Reinforcement," *Journal of the American Concrete Institute*, Proceedings Vol 61, No. 6 (June 1964), p 657.

⁹Swamy and Mangat.

¹⁰*Annual Book of ASTM Standards* (American Society for Testing and Materials [ASTM], May 1969), Part 31, p 1099.

¹¹E. T. Wessel, "State of the Art of the WOL Specimen for K_{Ic} Fracture Toughness Testing," *Engineering Fracture Mechanics*, Vol I (1968), p 77.

¹²A. A. Forzani, *Environmental Effects on Fiber Reinforced Concrete*, Unpublished M.S. Thesis (Clarkson College of Technology, 1972).

¹³M. J. Mathis, *Fracture Testing of Fiber Reinforced Concrete by Means of the Wedge Opening Loading Specimen*, Unpublished M.S. Thesis (Clarkson College of Technology, 1974).

Load-displacement curves were experimentally determined for notch depths of 2.25, 3, 4, and 5 in. (57.2, 76.2, 101.6, and 127.0 mm) and fiber contents of 1.0, 1.5, and 2.0 percent in the ambient condition of the laboratory. Compliance was then determined based on the specimen's original dimensions, and plotted versus the crack length to specimen length ratio for each fiber content. The compliance of the specimen was taken as the inverse slope of the stress-deformation curve.

The strain energy release rate, required to extend a crack for the ambient condition was compared with that for specimens subjected to 74, 113, 148, and 176 days of exposure to a flowing saltwater environment.

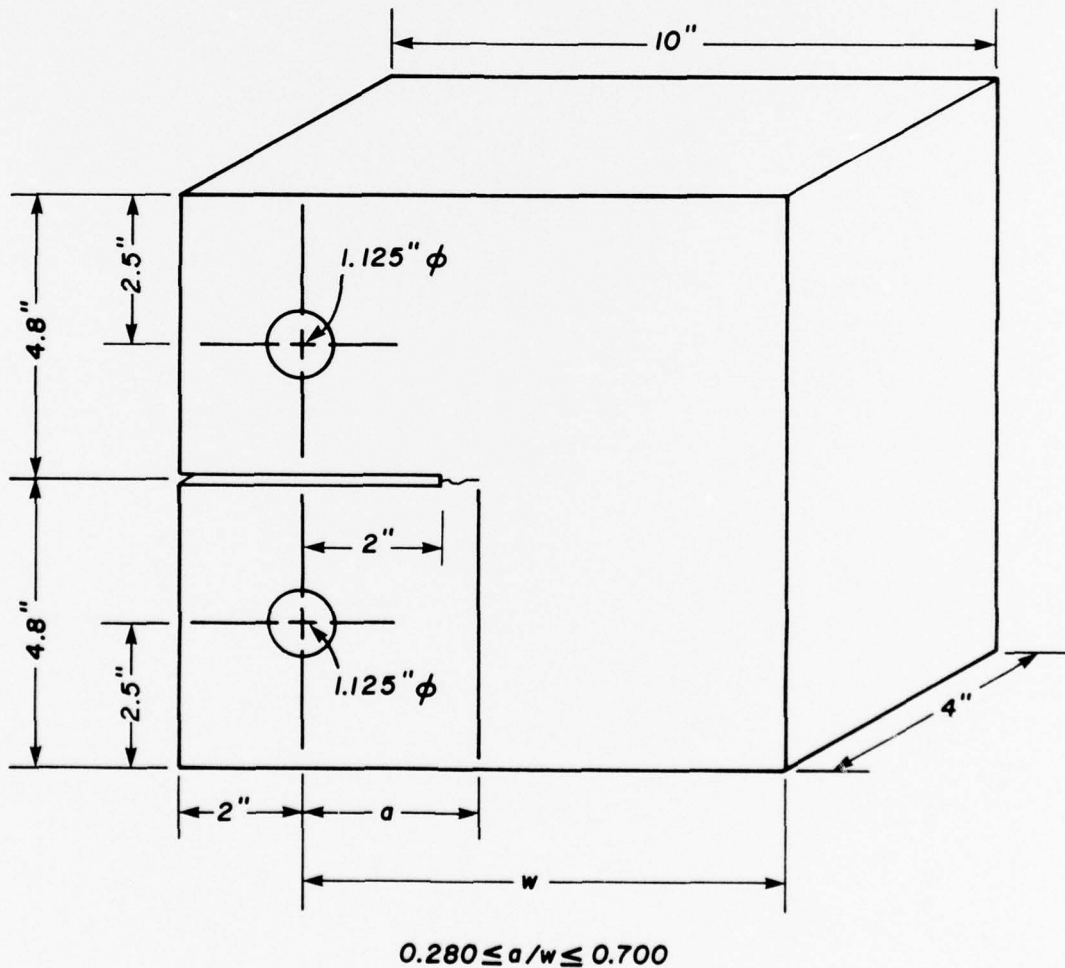


Figure 1. Modified WOL specimen. SI conversion factor: 1 in. = 2.54 cm.

The reduction in strain energy release rate is a measure of the effect of the flowing saltwater on the strength of the fiber-reinforced concrete, because the strain energy release rate can be directly related to the stress necessary to extend a crack.¹⁴

An added feature of the approach used was the experimental verification of the theoretically evaluated compliance curves for the WOL specimen.

¹⁴G. R. Irwin and J. A. Kies, "Critical Energy Rate Analysis of Fracture Strength," *Welding Journal*, Vol 33 (April 1954), p 193s.

2 TESTING PROGRAM

Test Specimen

The forms for specimen casting were constructed from steel plates 4 in. (101.6 mm) wide x 1/4 in. (6.4 mm) thick conforming to the dimensions in Figure 1 and mounted on a channel (12 in. wide by 20.7 lb [0.3 m by 9.4 kg]) base. Two channel section bases, each permitting mounting of four steel plate forms, were used. The loading pin holes were formed by fixing two tubes of 1 1/8 in. (28.6 mm) outside diameter aluminum coated with paraffin to the channel base.

The mix proportions given in Table 1 were adopted from a mix designed by the U.S. Army Construction Engineering Research Laboratory (CERL) for an overlay project at Fort Hood, TX. The sand used was a #1 dry silica sand supplied by Pennsylvania Glass Sand Corp. of Philadelphia, PA. The coarse aggregate was 3/8 in. (9.5 mm) peastone from Bicknell Brothers of Potsdam, NY. The cement was Portland High Early manufactured by Ciments Canada Lafarge Lte'e. Pozzoloth, a water-reducing admixture produced by Master Builders, was used at the rate of 743 ml/cu yd of mix (972 ml/m³). Tap water was employed throughout the process. U.S. Steel Fibercon fibers (Figure 2), 0.010 x 0.022 x 1.00 in. (0.254 x 0.559 x 25.4 mm), were added on a percentage by volume basis.

Table 1
Mix Design

A. Proportions Per Cubic Yard

Peastone	1351 lb (613 kg)
Sand	1351 lb (613 kg)
Cement	850 lb (386 kg)
Water.	510 lb (231 kg)
Water Reducer.	743 ml Pozzoloth
Fiber	
1.0%	136 lb (62 kg)
1.5%	204 lb (93 kg)
2.0%	272 lb (123 kg)

B. Sieve Analysis for #1 Silica Sand

Sieve No.	Opening, in.(mm)	% Retained	Cumulative % Retained
16	0.0460 (1.1684)	0.0	0.0
30	0.0232 (0.5893)	3.98	3.98
50	0.0116 (0.2946)	66.39	70.37
100	0.0058 (0.1473)	28.10	98.47
pan	0.0 (0.0)	1.53	-

$$\text{Fineness Modulus} = \frac{\sum \text{Cumulative \% Retained}}{100}$$

$$\text{Fineness Modulus} = 1.73$$

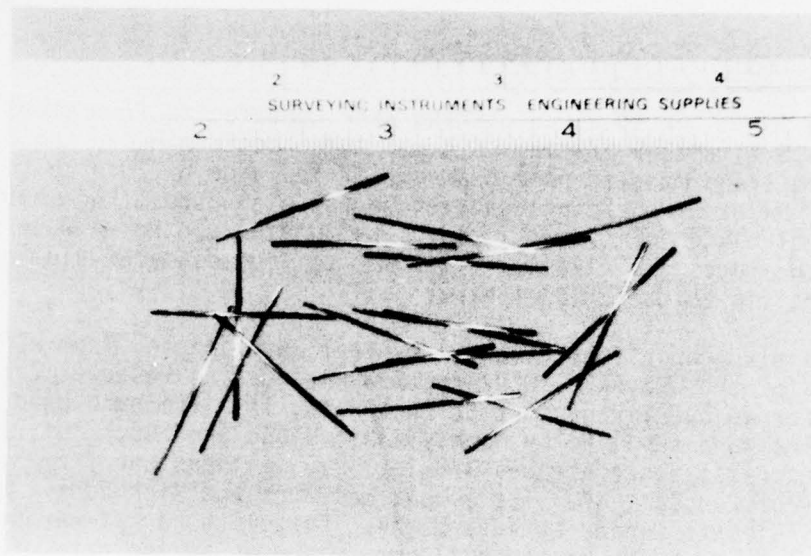


Figure 2. Steel fibers.

Specimen Casting Procedure

The concrete was mixed in a 2 cu ft (1.5 m³) electric-powered rotating drum mixer which had been moistened and allowed to drain. The mix constituents were weighed on a platform scale to an accuracy of 0.01 lb (0.01 kg). The liquid admixture, Pozzolith, was proportioned with a graduated cylinder to the nearest 0.1 ml.

The mixing sequence was as follows. First the peastone and then the sand were added to the mixer and allowed to mix for approximately 1 minute. Next, the cement was added and mixed for 1 minute. The water augmented with Pozzolith was slowly added while the mixer was rotating. With the mixer still rotating, the fibers were added by sifting them through a wire mesh basket to prevent segregation or "balling up" within the concrete mix. After the fibrous concrete was mixed for at least 3 minutes, or until thoroughly blended, it was placed in a wheelbarrow and transported to the forms.

The concrete was placed in the forms to a depth of 2 in. (50.8 mm), and the forms were vibrated externally by an electric vibrator. The forms were then filled with concrete and vibrated again. To insure random distribution and orientation of the fibers, the vibrator was not inserted into the mix. The surface of the specimens was then troweled smooth and covered with polyethylene. After the specimens cured in the forms for 72 hours, the forms were stripped and the specimens were placed in a moisture room where they cured for 25 days. One compression

cylinder conforming to American Society for Testing and Materials (ASTM) standards¹⁵ was cast for each batch of concrete mixed.

Control Specimen Testing Procedure

After the specimens were cured, groups of 16 specimens of each fiber content were removed from the moisture room and notched to depths of 2.25, 3, 4, and 5 in. (57.2, 76.2, 101.6, and 127.0 mm) with a masonry saw. A small crack was then propagated from the tip of the notch by means of the mechanical harness shown in Figure 3. India ink dye was injected into the crack to mark its depth. The crack was propagated so that the strain energy release rate (G_{IC}) would be determined for a sharp crack rather than a blunt notch as used in previous research.^{16,17}

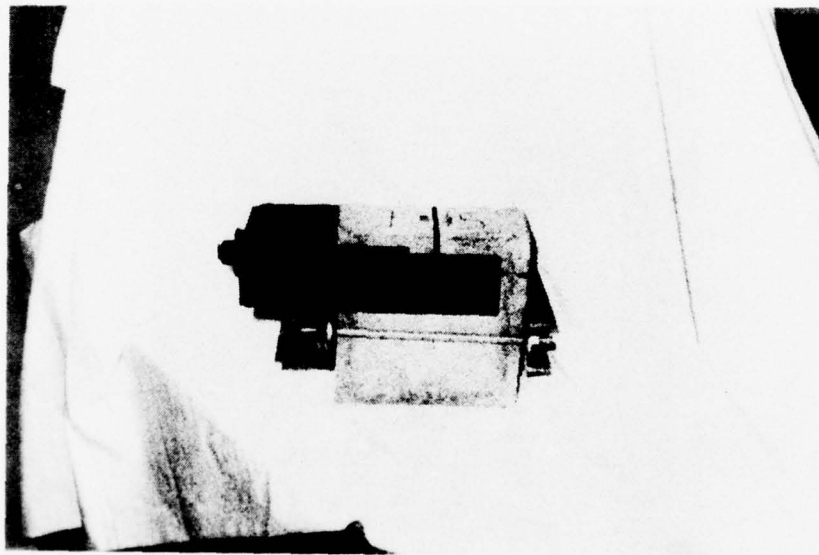


Figure 3. Mechanical cracking harness.

¹⁵Annual Book of ASTM Standards (ASTM, May 1969).

¹⁶Symposium on Fracture Toughness Testing and Its Applications, ASTM Special Technical Publication No. 381 (ASTM in cooperation with National Aeronautics and Space Administration [NASA], 1965).

¹⁷C. E. Turner, "Fracture Toughness and Specific Fracture Energy: A Re-Analysis of Results," *Materials Science and Engineering*, Vol 11 (May 1973), pp 275-282.

The specimens were tested in a Tinius Olsen Ucelotronic electro-mechanical testing machine (Figure 4) with autographic recorder (Figure 5). The recorder plotted the load applied to the specimens and the displacement across the front face of the notch in the direction of the applied load. The magnitude of the load was determined by a 12,000-lb (5443-kg) load cell in the electromechanical testing machine. The displacement was measured by the compliance gage shown in Figure 6; 0.1 in. (2.54 mm) of travel of the recording chart represented 0.000288 ± 0.000003 in. (0.007315 ± 0.000076 mm) of displacement. Figure 7 shows a schematic of the compliance gage, and Figure 8 shows the control specimens prepared for testing.



Figure 4. Electromechanical testing machine.

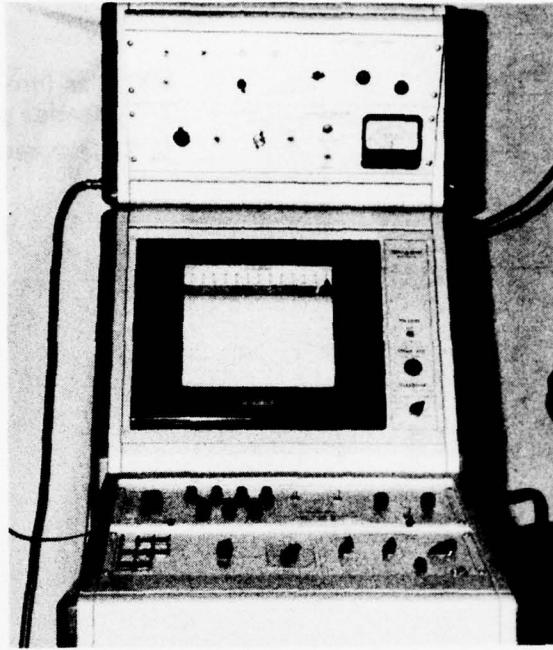


Figure 5. Autographic recorder.

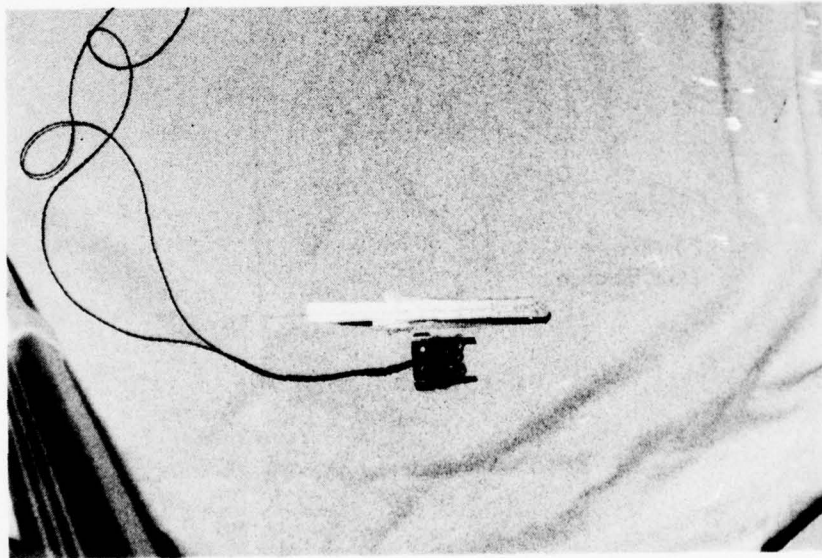
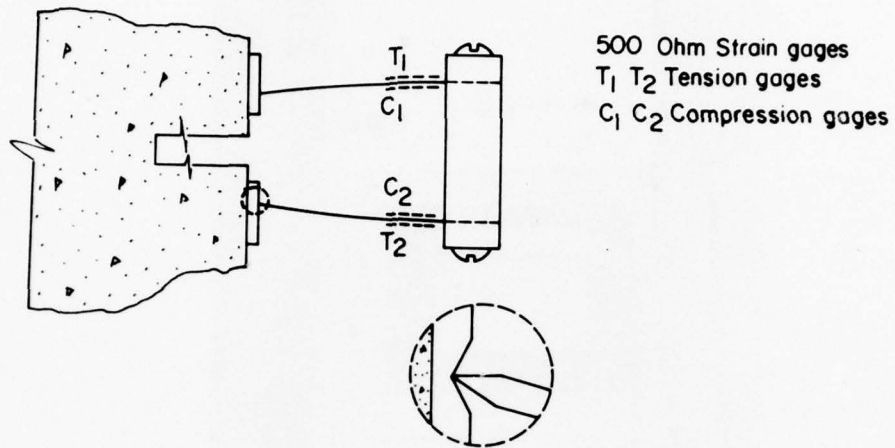
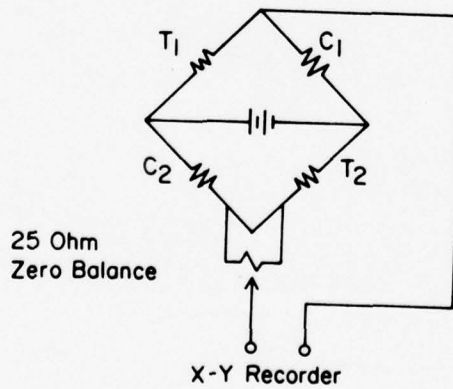


Figure 6. Compliance gage.

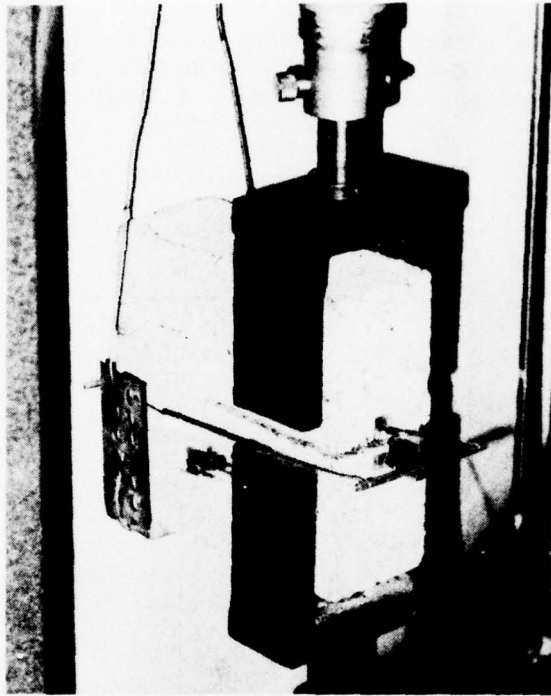


a. Compliance gage mounted on specimen.

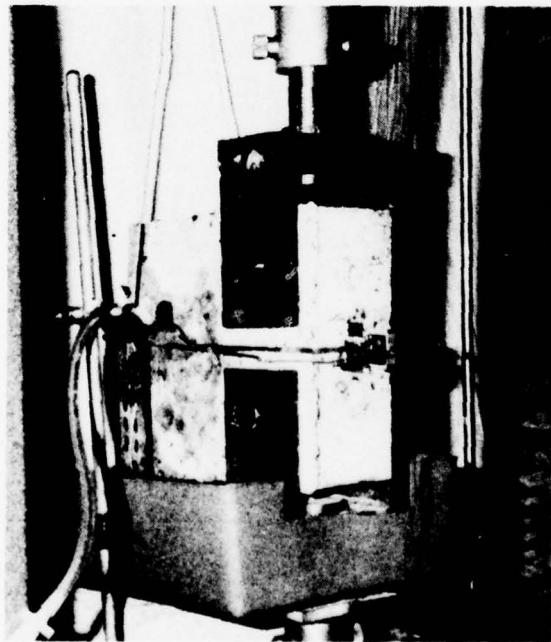


b. Bridge measurement.

Figure 7. Schematic of compliance gage.



a. Compliance specimen.



b. Flushing of environmental specimen.

Figure 8. Specimens prepared for testing.

Each specimen was loaded to failure, and the inverse slope of the linear portion of the load-displacement curve was computed as the compliance of the specimen. Figure 9 shows a typical load-displacement relationship.

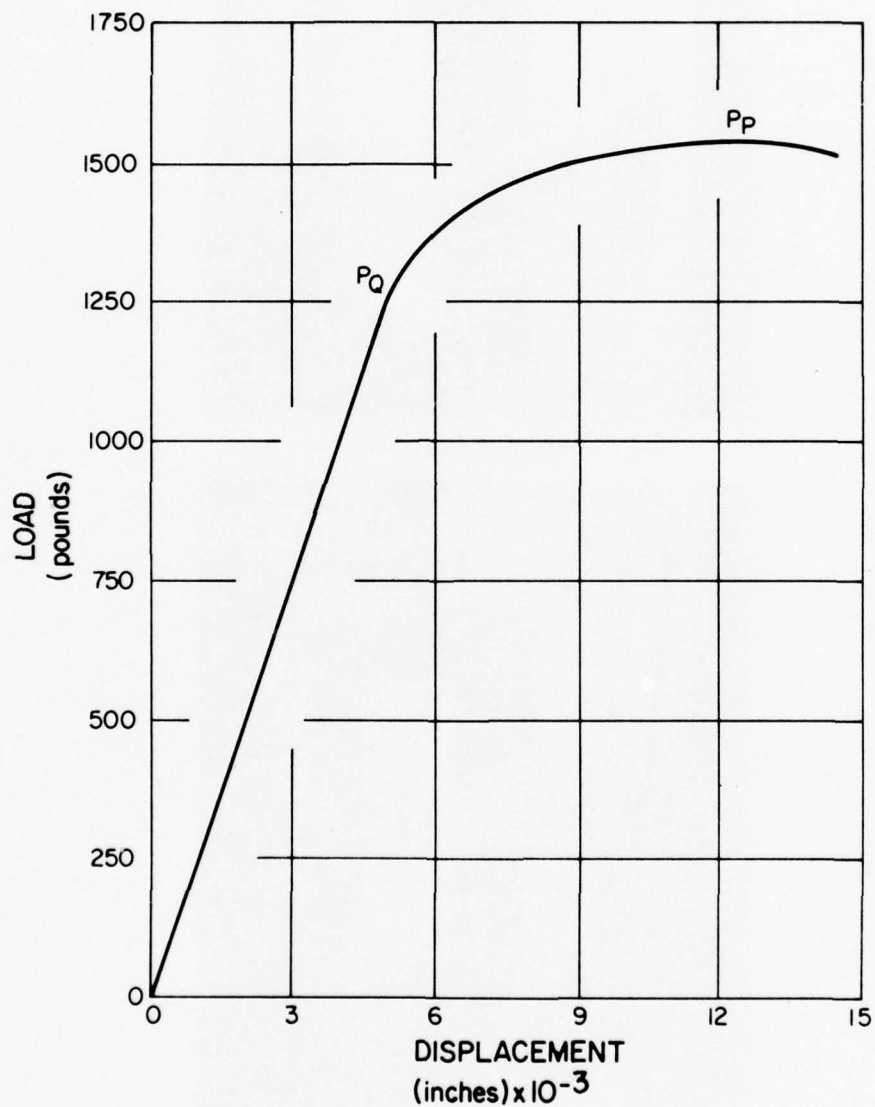


Figure 9. Typical load-displacement relationship. SI conversion factors: 1 in. = 25.4 mm; 1 lb = 0.4536 kg.

Environmental Specimen Testing Procedure

The environmental specimens were cast and cured in the same manner as the control specimens. All specimens to be exposed to the saltwater environment had a sawed notch depth of 4 in. (101.6 mm), with a sharp crack propagated from the notch tip. The notch was held open by a system of wooden wedges forced into the front face of the notch. The purpose of the wooden wedges was to create a region of high stress concentration at the tip of the sharp crack. The specimens were then placed in the environmental tank (Figure 10) where the crack tips were subjected to continuous flushing of artificial saltwater for varying exposure durations. The artificial saltwater solution was made by adding 3.5 percent sodium chloride and 0.5 percent magnesium sulfate by weight to distilled water.¹⁸ The salt content in solution was monitored weekly and adjusted if necessary. The pH, conductivity, and temperature of the solution were monitored weekly throughout the experiment.

The artificial saltwater was delivered directly to the notch of each specimen by a 0.25-in. (6.4-mm) inside diameter Tygon tube. The tubes were individually secured to the spigots at the base of a tank which provided 18 in. (0.5 m) of constant hydrostatic head. The flow rate through each tube was held constant at 0.15 gal/minute (0.6 l/minute) by using a clamp flow restriction located on each tube. The entire environmental tank was covered with a polyethylene sheet to minimize evaporating losses.

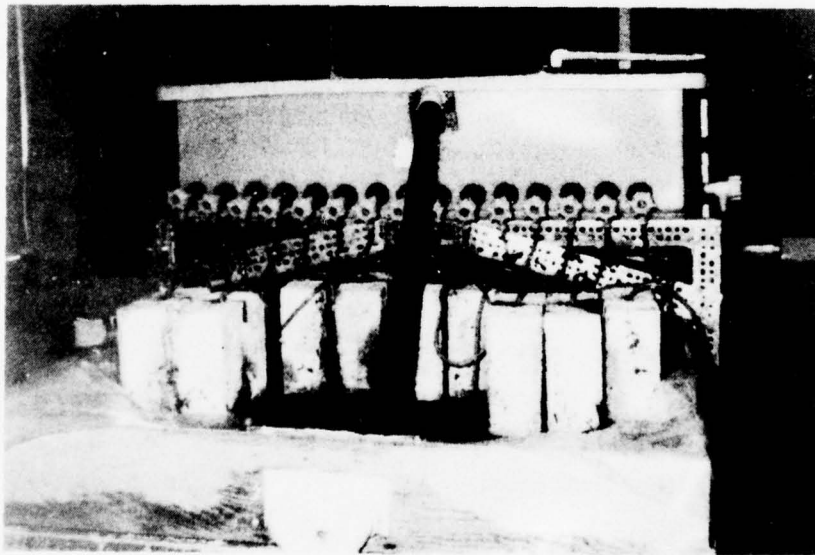


Figure 10. Environmental exposure tank.

¹⁸H. Woods, *Durability of Concrete Construction*, ACI Monograph #4 (American Concrete Institute [ACI], Iowa State University Press, 1968), p 137.

Three specimens of each fiber content--1.0, 1.5, and 2 percent--were exposed to the saltwater environment for 74, 113, 148, and 176 days. At the end of each time interval, specimens were removed from the environmental tank and loaded to failure on the electromechanical testing machine.

Compliance Analysis

A modified compliance testing procedure was used in determining the critical strain energy release rates for both the control and environmentally exposed specimens. Compliance testing relates to the load deflection characteristics of a material with the associated external energy changes or work done on the specimen.¹⁹ The compliance is the inverse spring constant of the material. The critical strain energy release rate is related to the specimen compliance by Eq 1:

$$G_c = 0.5(P_Q B)^2 \frac{dC}{da} \quad [\text{Eq 1}]$$

where: G_c = the critical strain energy release

B = the width of the specimen

P_Q = the load at which crack propagation initiates

$\frac{dC}{da}$ = the slope of the compliance curve at the particular crack length being analyzed.

For a given fiber content, the specimen compliance was plotted as a function of the crack length ratio, obtained by dividing the crack length by the specimen length. The modified polynomial least square curve fit computer program in Appendix B was used to fit a curve to the data. The work rate necessary to extend the crack was then determined by the experimental relationship:

$$G_{IC} = \frac{0.5 \left[\frac{P_Q}{B} \right]^2 \frac{dc}{d(a/w)}}{w} \quad [\text{Eq 2}]$$

where G_{IC} = the work rate required to extend the crack a unit distance

B = the specimen width

P_Q = the load at which the load-deflection curve deviates from linearity

¹⁹J. F. Knott, *Fundamentals of Fracture Mechanics* (Butterworths, 1973), p 105.

$\frac{dc}{d(a/w)}$ = the slope of the compliance curve at the particular crack length ratio being evaluated

w = the specimen length.

Two modifications of the polynomial least square fit were made to analyze the data. At a crack length ratio of zero, the compliance was set equal to an approximate value of the inverse of the modulus of elasticity for the material. Furthermore, the coefficient of the first-order term in the polynomial was forced to zero on the a priori basis that G_{IC} would of necessity be zero for zero crack length.²⁰

After loading the specimens to failure, the G_{IC} values were computed using Eq 1, where P_0 was the load at which the load-deflection curve of the environmentally exposed specimens deviated from linearity.

To verify the correctness of the experimental compliance curves, an analytical solution for the stress intensity factor, K, was employed. This analytical relationship is:²¹

$$K = \frac{P_0(a/w)^{1/2}Y}{B(w^{1/2})} \quad [\text{Eq 3}]$$

where Y = a polynomial obtained by boundary collection of the Williams stress function.^{22,23}

For the WOL specimen used, Y is given as

$$Y = 29.6 - 185.5(a/w) + 655.7(a/w)^2 - 1017(a/w)^3 + 638.9(a/w)^4 \quad [\text{Eq 4}]$$

The compliance (C) can be related to the polynomial Y in the following manner:²⁴

$$C = \frac{L[f(a/w)]}{wBE} \quad [\text{Eq 5}]$$

²⁰J. E. Srawley, M. H. Jones, and B. Gross, *Experimental Determination of the Dependence of Crack Extension Force on Crack Length for a Single Edge Notch Tension Specimen*, NASA Technical Note D 2396 (NASA, August 1964).

²¹J. D. Desai and W. W. Gerberich, "Analysis of Incremental Cracking by the Stress Wave Emission Technique," *Engineering Fracture Mechanics*, Vol 7 (Pergamon Press, 1975), p 156.

²²Desai and Gerberich.

²³B. Gross, J. E. Srawley, and W. P. Brown, *Stress Intensity Factors for a Single Edge Notch Tension Specimen by Boundary Collocation of a Stress Function*, NASA Technical Note D 2395 (NASA, August 1964).

²⁴Desai and Gerberich.

where L = the distance between points of application
of the tensile force

$f(a/w)$ = proportional to Y

E = the modulus of elasticity.

The relationship for the specimen geometry (Figure 1) is

$$C = \frac{L}{wBE} [2.7(a/w)^{1/2}Y^2] \quad [\text{Eq 6}]$$

where the constant 2.7 was changed from 0.8 as given by Desai and Gerberich.

An attempt was made to generate two compliance values from each specimen. The specimen was loaded until the maximum sustainable load for a particular crack length, P_p , was reached. A methyl red dye was then injected into the crack, and the specimen was unloaded. After the dye had dried, the specimen was again loaded to failure and the compliance determined in the same manner as before.

3 RESULTS

For all fiber contents, the exposure to the artificial saltwater environment decreased the strain energy release rate required for crack propagation (Table 2). Figure 11 shows a typical relationship between G_{IC} and exposure. The effect of the saltwater was less pronounced with each increase in fiber concentration. For the 1 percent fiber specimens, the critical strain energy release rate decreased from 0.540 (in.-lb)/sq in. (94.6 m-N/m²) for the ambient condition to 0.388 (in.-lb)/sq in. (68.0 m-N/m²) after 74 days of exposure, a drop of 28 percent. During the remaining 102 days of exposure, the G_{IC} value decreased to 0.356 (in.-lb)/sq in. (62.3 m-N/m²), an additional decrease of 5.92 percent with more than 100 percent increase in exposure time. The G_{IC} values for the 1.5 percent fiber specimens decreased from 0.850 (in.-lb)/sq in.

Table 2
Critical Strain Energy Release
Rates of Environmental Specimens

1.0 Percent Fiber					
a/w*	Exposure Days	P _Q lb (kg)	G _{IC} (in.-lb)/sq in. (m-N/m ²)	P _p lb (kg)	G _{IC} (in.-lb)/sq in. (m-N/m ²)
0.566	74	760 (345)	0.388 (68.0)	805 (365)	0.435 (78.8)
0.564	74	780 (354)	0.403 (70.6)	870 (394)	0.502 (87.9)
0.516	74	890 (404)	0.373 (65.3)	1025 (465)	0.495 (86.7)
			Avg: 0.388 (68.0)	Avg: 0.477 (83.5)	
0.516	113	890 (404)	0.373 (65.3)	968 (439)	0.442 (77.4)
0.512	113	913 (414)	0.382 (66.9)	1210 (549)	0.670 (117.3)
0.506	113	1000 (455)	0.438 (76.7)	1193 (541)	0.633 (110.9)
			Avg: 0.398 (69.7)	Avg: 0.582 (101.9)	
0.520	148	870 (394)	0.367 (64.3)	960 (435)	0.477 (83.5)
0.513	148	890 (404)	0.365 (63.9)	955 (433)	0.421 (73.7)
0.505	148	930 (422)	0.362 (63.4)	1135 (515)	0.540 (94.6)
			Avg: 0.365 (63.9)	Avg: 0.479 (83.9)	
0.539	176	800 (363)	0.356 (62.3)	1035 (469)	0.596 (104.4)
0.524	176	850 (386)	0.361 (63.2)	1255 (569)	0.787 (137.8)
0.508	176	890 (404)	0.352 (61.6)	1170 (531)	0.608 (119.1)
			Avg: 0.356 (62.3)	Avg: 0.664 (116.3)	

*a is the distance from the center of the loading pin holes to the bottom of the sawed notch plus the length of the mechanically induced crack; w is the width of the specimen, which is a constant.

Table 2 (cont'd)

1.5 Percent Fiber

0.531	74	1200 (544)	0.837 (146.6)	1660 (753)	1.601 (280.3)
0.525	74	1220 (553)	0.809 (141.7)	1990 (862)	1.996 (349.6)
0.523	74	1100 (499)	0.658 (115.2)	1160 (526)	0.732 (128.2)

Avg: 0.768 (134.5)

Avg: 1.443 (252.7)

0.518	113	1180 (535)	0.726 (127.1)	1620 (735)	1.369 (239.7)
0.512	113	1300 (590)	0.838 (146.8)	1700 (771)	1.432 (250.8)
0.506	113	1300 (590)	0.795 (139.2)	1740 (789)	1.425 (249.6)

Avg: 0.786 (137.7)

Avg: 1.409 (246.8)

0.535	148	1060 (481)	0.675 (118.2)	1170 (531)	0.822 (144.0)
0.510	148	1220 (553)	0.725 (127.0)	1440 (653)	1.010 (176.9)
0.506	148	1260 (572)	0.747 (130.8)	1700 (771)	1.360 (238.2)

Avg: 0.716 (25.4)

Avg: 1.064 (186.3)

0.547	176	1030 (467)	0.701 (122.8)	1040 (472)	0.715 (125.2)
0.520	176	1160 (526)	0.714 (125.0)	1750 (794)	1.608 (281.6)
0.516	176	1130 (513)	0.655 (114.7)	1860 (844)	1.744 (305.4)

Avg: 0.690 (120.8)

Avg: 1.356 (237.5)

2.0 Percent Fiber

0.531	74	1120 (508)	0.699 (122.4)	1440 (653)	1.155 (202.3)
0.510	74	1760 (798)	1.351 (236.6)	2155 (977)	2.026 (354.8)
0.508	74	1590 (721)	1.076 (188.4)	2035 (923)	1.763 (308.8)

Avg: 1.042 (182.5)

Avg: 1.648 (288.6)

0.506	113	1560 (708)	1.011 (177.0)	1960 (889)	1.596 (279.5)
0.506	113	1500 (680)	0.935 (163.7)	2110 (957)	1.849 (323.8)
0.504	113	1580 (717)	1.012 (177.2)	1730 (785)	1.213 (212.4)

Avg: 0.986 (172.7)

Avg: 1.553 (272.0)

0.522	148	1340 (608)	0.903 (158.1)	1600 (726)	1.288 (225.6)
0.517	148	1430 (649)	0.930 (162.9)	2060 (934)	2.013 (352.5)
0.512	148	1460 (662)	1.177 (206.1)	1790 (812)	1.770 (310.0)

Avg: 1.003 (175.7)

Avg: 1.690 (296.0)

0.521	176	1400 (635)	0.974 (170.6)	1900 (862)	1.795 (314.4)
0.510	176	1460 (662)	0.930 (162.9)	1870 (848)	1.525 (267.1)
0.508	176	1550 (703)	1.023 (179.2)	2220 (1007)	2.098 (367.4)

Avg: 0.976 (170.9)

Avg: 1.806 (316.3)

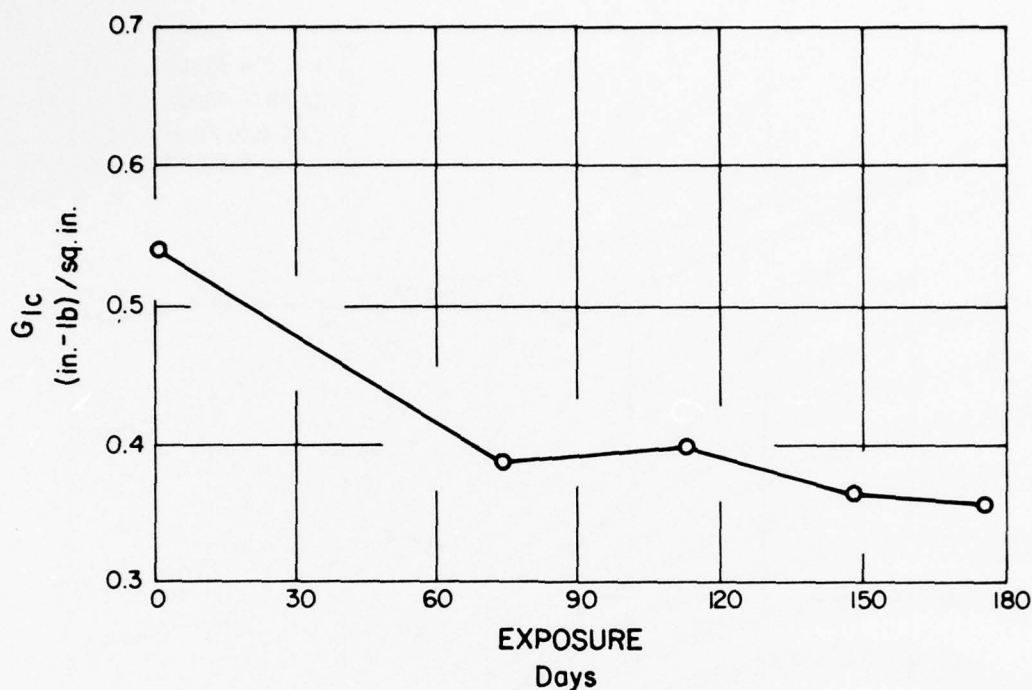


Figure 11. Critical strain energy release rate for 1.0 percent fiber content. SI conversion factor: 1 (in.-lb)/sq in. = 175.13 m-N/m².

(148.9 m-N/m²) for the ambient condition to a 0.768 (in.-lb)/sq/in. (135.5 m-N/m²) after 74 days of exposure, a drop of 9.65 percent. After 176 days of exposure, the G_{IC} value decreased to 0.690 (in.-lb)/sq in. (120.8 m-N/m²), for a total decrease in critical strain energy release rate of 18.82 percent. The G_{IC} values for the 2 percent fiber specimens decreased from 1.10 (in.-lb)/sq in. (192.6 m-N/m²) for the ambient condition to 1.04 (in.-lb)/sq in. (182.1 m-N/m²) after 74 days of exposure. For the remaining 102 days of exposure, the G_{IC} value dropped to 0.976 (in.-lb)/sq in. (170.9 m-N/m²) decrease of 1.3 percent for the entire duration of exposure.

As the fiber content increased, the specimens retained a greater percentage of their ambient G_{IC} values for any given duration of exposure. Figure 12 shows the effect of exposure time on the rate of G_{IC} values for the three fiber concentrations. A student 't' test was made for the average G_{IC} to establish if there was a statistically significant change in G_{IC} for each succeeding increment of exposure. Table 3 shows the results. If the absolute value of t calculated is greater than the table t_{90} value, then G_{IC} changed significantly from one exposure level to another.

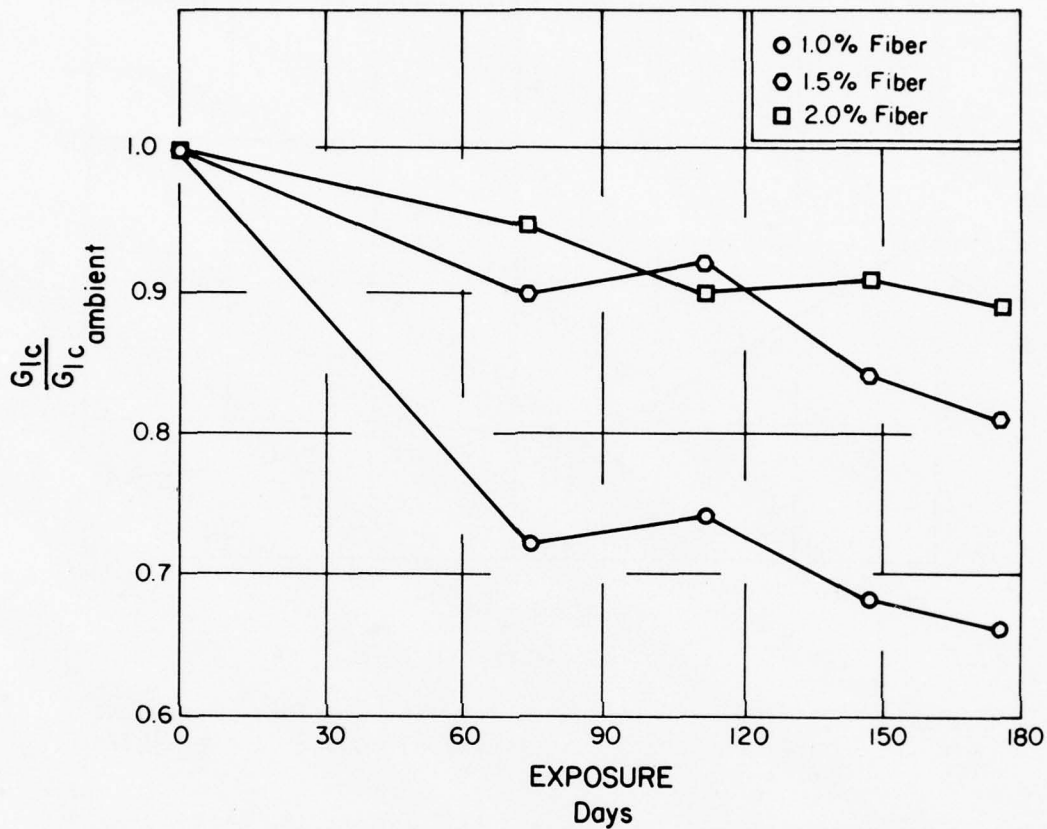


Figure 12. Relative critical strain energy release rates.

For each fiber content, the polynomial least square curve fit for the compliance function resulted in a fourth-order equation. These equations are:

1.0 percent fiber content

$$C = [663.6875(a/w)^4 - 492.1875(a/w)^3 + 144.6875(a/w)^2 + 0.2441] \times 10^{-6} \quad [\text{Eq 7}]$$

1.5 percent fiber content

$$C = [871.75(a/w)^4 - 644.75(a/w)^3 + 162.3125(a/w)^2 + 0.6975] \times 10^{-6} \quad [\text{Eq 8}]$$

2.0 percent fiber content

$$C = [1634.8125(a/w)^4 - 1480.3125(a/w)^3 + 391.75(a/w)^2 + 0.0349] \times 10^{-6} \quad [\text{Eq 9}]$$

Table 3
Student 't' Test for Average G_{IC} Values

1 Percent Fiber

Exposure	G_{IC}	Std. Dev.	t* Calculated	t_{90} *
0	0.540	0.064		
74	0.388	0.015	3.98	1.77
113	0.398	0.035	-0.455	2.13
148	0.365	0.003	1.63	2.13
176	0.356	0.005	2.67	2.13

1.5 Percent Fiber

Exposure	G_{IC}	Std. Dev.	t Calculated	t_{90}
0	0.850	0.074		
74	0.768	0.096	1.63	1.77
113	0.786	0.057	-0.28	2.13
148	0.716	0.037	1.78	2.13
176	0.690	0.031	0.933	2.13

2 Percent Fiber

Exposure	G_{IC}	Std. Dev.	t Calculated	t_{90}
0	1.10	0.249		
74	1.042	0.327	0.342	1.77
113	0.986	0.044	0.294	2.13
148	1.003	0.151	-0.187	2.13
176	0.976	0.047	0.296	2.13

*If the absolute value of t calculated is greater than the table t_{90} value, then G_{IC} changed significantly from one exposure level to another.

Table 4 shows the compliance and load results for the control specimens. The results of the curve fit are shown in Figures 13, 14, and 15 and in the computer printout in Appendix B.

For all fiber contents, P_0 and P_p generally decreased with increasing notch depth ratios. The critical strain energy release rates for the control specimens (Table 5) remained relatively constant within each fiber content. Specimens with 1.0 percent fiber content and a/w ratios in excess of 0.600 were the exceptions; values for these four specimens were internally consistent, but were 19 percent lower than the results obtained for shallow notch depths. Throughout the fiber content range, an increase in fiber content of 0.5 percent produced a corresponding increase in G_{IC} value of approximately 0.3 (in.-lb)/sq in. (5.25 m-N/m²).

Of the control specimens tested, four of the 48 data points obtained were rejected because the cracks did not propagate perpendicular to the plane of loading. The skewed cracks induced erroneous compliance values which were omitted from the data analysis.

The results of the compression cylinder tests (Table 6) were consistent within each fiber content. The respective compressive stresses at failure were 6070, 5589, and 5932 psi (41 883, 38 564, and 40 931 kN/m²) for fiber contents of 1.0, 1.5, and 2.0 percent.

Extremely good correlation between experimental and analytical compliance values was maintained throughout the experiment. The magnitude of the first derivative of the experimental compliance curves and the analytical relationship of Eq 6 differ by a maximum of 5 percent throughout the range of a/w values used (Figure 16).

The pH of the saltwater solution increased from 7.2 to 8.8 within the first 4 hours of environmental exposure (Table 7). A gradual increase in pH was noted during the next 37 days of exposure, until equilibrium was attained at a pH of roughly 9.65. The conductivity of the solution maintained a relatively constant value of approximately 48 000 μ mhos/cm². The temperature of the saltwater environment remained between 69° and 76°F (21° and 24°C). Although a polyethylene sheet covered the entire environmental tank, evaporation losses were observed to be approximately 1.5 gal (5.7 ℓ) of water per month.

Table 4
Compliance, Crack Onset, and Ultimate
Loads of Control Specimens

1 Percent Fiber

Specimen No.	a/w	C (sq in./lb)x10 ⁻⁶ [(m ² /kN)x10 ⁻⁶]	P _Q lb (kg)	P _P lb (kg)
4-10-5	0.680	58.68 (8.51)	570 (259)	628 (285)
3-10-5	0.672	47.83 (6.94)	616 (279)	672 (305)
5-10-5	0.664	49.20 (7.13)	557 (253)	637 (289)
1-10-5	0.640	39.27 (5.69)	600 (272)	721 (327)
6-10-4	0.563	30.61 (4.44)	990 (449)	1030 (467)
2-10-4	0.555	24.28 (3.52)	890 (404)	955 (433)
3-10-4	0.547	20.50 (2.97)	1080 (490)	1230 (509)
1-10-4	0.523	16.58 (2.40)	1042 (473)	1319 (598)
1-10-3	0.422	9.73 (1.42)	1420 (644)	1540 (699)
7-10-2	0.410	9.67 (1.40)	1670 (757)	1890 (857)
2-10-3	0.398	10.13 (1.47)	1460 (726)	1640 (744)
6-10-3	0.398	8.97 (1.30)	1450 (658)	1545 (701)
7-10-2	0.390	8.44 (1.22)	1850 (839)	1920 (871)
5-10-3	0.387	7.18 (1.04)	1510 (685)	1865 (846)
7-10-2	0.360	7.53 (1.09)	2230 (1016)	2260 (1025)
7-10-2	0.330	5.64 (0.82)	1770 (803)	2370 (1075)

1.5 Percent Fiber

1-15-5	0.688	59.90 (8.69)	605 (274)	705 (320)
4-15-5*	0.66	32.32 (4.69)	670 (304)	895 (406)
5-15-5	0.656	56.60 (8.21)	800 (363)	890 (404)
6-15-5	0.656	48.14 (6.98)	780 (354)	940 (426)
2-15-4	0.531	18.13 (2.63)	1010 (458)	1115 (506)
6-15-4	0.523	18.62 (2.70)	1222 (554)	1892 (858)
5-15-4	0.521	17.39 (2.52)	1310 (594)	1535 (696)
3-15-4	0.521	17.47 (2.53)	1320 (599)	1850 (839)
3-15-3	0.450	9.90 (1.44)	1500 (680)	1575 (714)
4-15-3	0.438	8.69 (1.26)	1700 (771)	2775 (1259)
2-15-3*	0.438	22.96 (3.33)	1300 (590)	1420 (644)
7-15-2	0.435	9.28 (1.35)	1850 (839)	2775 (1259)
1-15-3	0.398	8.50 (1.23)	1560 (708)	2380 (1080)
7-15-2	0.380	6.96 (1.01)	2400 (1089)	3550 (1610)
7-15-2	0.380	8.00 (1.16)	2300 (1043)	2725 (1236)
7-15-2	0.281	5.27 (0.76)	2550 (1157)	2800 (1270)

2.0 Percent Fiber

6-20-5*	0.727	129.15 (18.73)	630 (286)	670 (304)
4-20-5	0.680	63.31 (9.18)	822 (373)	unk.
3-20-5	0.672	62.32 (9.04)	870 (395)	1066 (484)
5-20-5	0.656	55.10 (7.99)	890 (404)	1055 (479)
5-20-4	0.551	22.08 (3.20)	1200 (544)	1444 (655)
2-20-4	0.531	17.01 (2.47)	1400 (635)	2256 (1023)
3-20-4	0.516	18.13 (2.63)	1400 (635)	2010 (912)
1-20-4	0.516	14.97 (2.17)	1560 (708)	2225 (1009)
7-20-2	0.512	16.14 (2.34)	1750 (794)	2600 (1179)
6-20-3	0.422	13.12 (1.90)	2650 (1202)	3070 (1393)
3-20-3	0.406	11.19 (1.62)	2300 (1043)	2650 (1202)
5-20-3	0.406	10.29 (1.49)	2510 (1139)	2860 (1297)
2-20-3	0.391	8.50 (1.23)	2100 (953)	3325 (1508)
7-20-2	0.387	10.05 (1.46)	3550 (1610)	3850 (1746)
7-20-2	0.313	6.74 (0.98)	3600 (1632)	3850 (1746)
7-20-2**	-	23.04 (3.34)	2350 (1066)	2700 (1225)

*Rejected based on physical observation. Crack did not propagate perpendicular to the plane of loading.
**Rejected based on physical observation. Neither crack initiation nor propagation was perpendicular to the plane of loading. The angle of crack incidence was so severe that a valid a/w ratio could not be obtained.

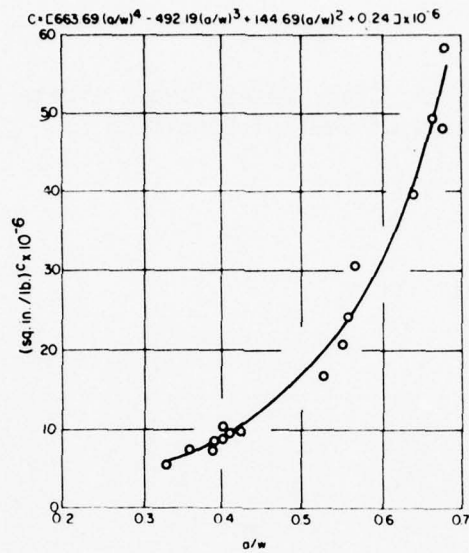


Figure 13. Compliance curve fit for 1.0 percent fiber content.
SI conversion factor: 1 sq in./lb = 0.14 m²/kN.

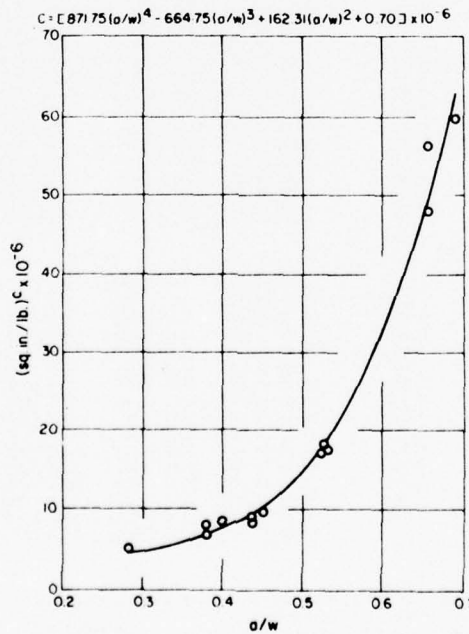


Figure 14. Compliance curve for 1.5 percent fiber content.
SI conversion factor: 1 sq in./lb = 0.14 m²/kN.

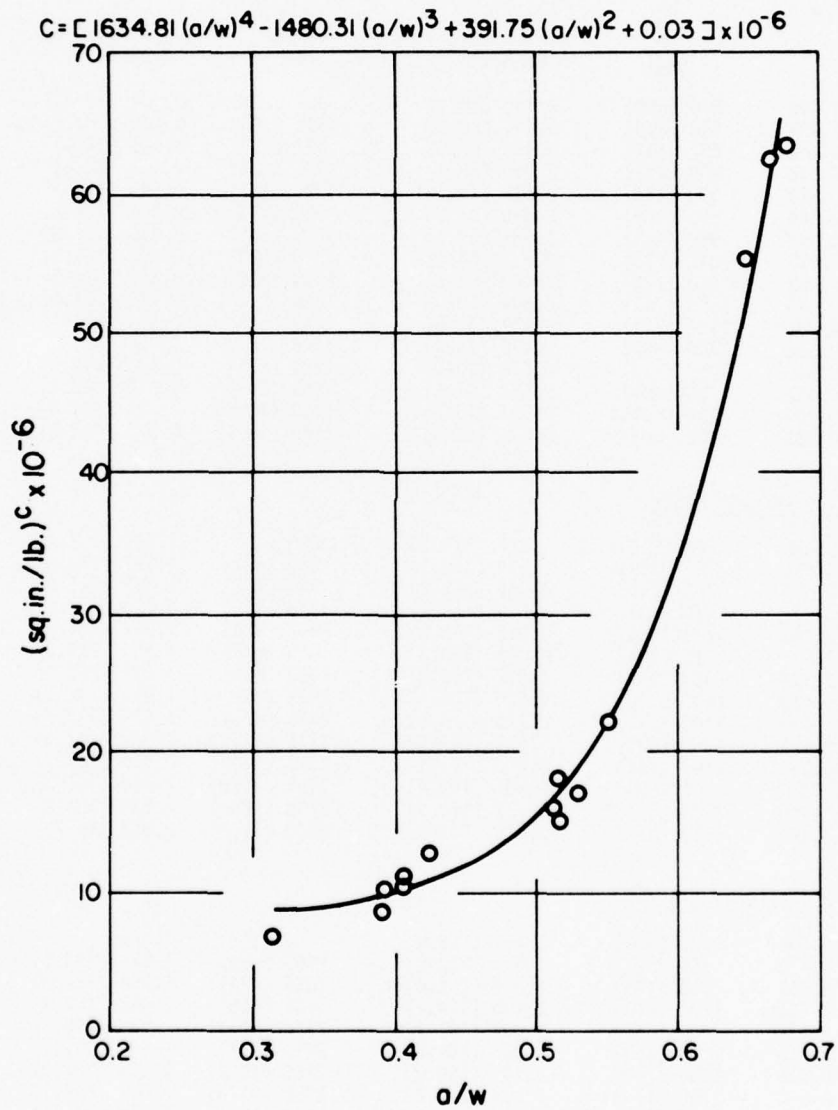


Figure 15. Compliance curve fit for 2.0 percent fiber content.
 SI conversion factor: 1 sq in./lb = 0.14 m²/kN.

Table 5
Critical Strain Energy
Release Rate of Control Specimens

1.0 Percent Fiber

a/w	P _Q lb (kg)	G _{IC} (in.-lb)/sq in. (m-N/m ²)	P _P lb (kg)	G _{IC} (in.-lb)/sq in. (m-N/m ²)
0.680	570 (259)	0.443 (77.6)	628 (285)	0.538 (94.2)
0.672	616 (279)	0.495 (86.7)	672 (305)	0.589 (103.2)
0.664	557 (253)	0.386 (67.6)	637 (289)	0.505 (88.4)
0.640	600 (272)	0.389 (68.1)	721 (327)	0.562 (98.4)
0.563	990 (449)	0.645 (113.0)	1030 (467)	0.698 (122.2)
0.555	890 (404)	0.525 (91.9)	955 (433)	0.604 (105.8)
0.547	980 (445)	0.566 (99.1)	1230 (509)	0.891 (156.0)
0.523	1042 (473)	0.539 (94.4)	1319 (598)	0.863 (151.1)
0.422	1460 (726)	0.490 (85.8)	1540 (699)	0.545 (95.4)
0.410	1670 (757)	0.584 (102.3)	1890 (857)	0.748 (131.0)
0.398	1580 (717)	0.477 (83.5)	1640 (744)	0.514 (90.0)
0.398	1500 (680)	0.430 (75.3)	1545 (701)	0.456 (78.8)
0.390	1850 (839)	0.616 (107.9)	1920 (871)	0.633 (110.9)
0.387	1780 (807)	0.557 (97.5)	1865 (846)	0.612 (107.2)
0.360	2230 (1016)	0.597 (104.6)	2260 (1025)	0.741 (129.8)
0.330	1770 (803)	0.376 (65.8)	2370 (1075)	0.675 (118.2)

1.5 Percent Fiber

0.688	690 (313)	0.826 (144.7)	795 (361)	1.097 (192.1)
0.656	800 (363)	0.914 (160.1)	890 (404)	1.131 (198.3)
0.656	780 (354)	0.869 (152.2)	940 (426)	1.262 (221.0)
0.531	1170 (531)	0.839 (146.9)	1315 (596)	1.200 (210.2)
0.523	1222 (554)	0.812 (142.2)	1892 (858)	1.947 (341.0)
0.521	1310 (594)	0.918 (160.8)	1535 (696)	1.260 (220.7)
0.521	1320 (599)	0.932 (163.2)	1850 (839)	1.830 (320.5)
0.450	1600 (726)	0.720 (126.1)	1975 (896)	1.097 (192.1)
0.438	1700 (771)	0.723 (126.6)	2775 (1259)	1.925 (337.1)
0.435	1850 (839)	0.831 (145.5)	2775 (1259)	1.869 (327.3)
0.398	1560 (708)	0.406 (71.1)	2380 (1080)	0.946 (165.7)
0.380	2400 (1089)	0.801 (140.4)	3550 (1610)	1.753 (306.5)
0.380	2300 (1043)	0.736 (128.9)	2725 (1236)	1.033 (180.9)
0.281	2550 (1157)	0.425 (74.4)	2800 (1270)	0.512 (89.7)

2.0 Percent Fiber

0.680	822 (373)	1.415 (247.8)	unk.	unk.
0.672	870 (395)	1.496 (262.0)	1066 (484)	2.247 (393.5)
0.656	890 (404)	1.390 (243.4)	1055 (479)	1.954 (342.2)
0.551	1200 (544)	0.996 (174.4)	1444 (655)	1.442 (252.5)
0.531	1400 (635)	1.092 (191.2)	2256 (1023)	2.836 (496.7)
0.516	1500 (680)	1.055 (184.8)	2010 (912)	1.894 (331.7)
0.516	1560 (708)	1.141 (199.8)	2225 (1009)	2.321 (387.0)
0.512	1750 (794)	1.369 (239.8)	2600 (1179)	3.021 (529.1)
0.422	2650 (1202)	0.857 (150.1)	3070 (1393)	1.151 (201.6)
0.406	3000 (1361)	0.838 (146.8)	3450 (1565)	1.108 (194.0)
0.406	3050 (1383)	0.866 (151.7)	3420 (1551)	1.089 (190.7)
0.391	3360 (1524)	0.817 (143.1)	3680 (1669)	0.980 (171.6)
0.387	3550 (1610)	0.855 (149.7)	3850 (1746)	1.005 (176.0)
0.313	3660 (1632)	0.577 (101.1)	3850 (1746)	0.659 (115.4)

Table 6
Compressive Strength Cylinders

1.0 Percent Fiber

<u>Cylinder</u>	<u>Stress at Failure, psi (kN/m²)</u>
1-10	6047 (41 724)
2-10	6132 (42 311)
3-10	5913 (40 800)
4-10	6115 (42 194)
5-10	6330 (43 677)
6-10	5535 (38 192)
7-10	6415 (44 264)

Average maximum compressive stress: 6070 psi (41 883 kN/m²)
Coefficient of variation: 4.78 percent

1.5 Percent Fiber

<u>Cylinder</u>	<u>Stress at Failure, psi (kN/m²)</u>
1-15	6062 (41 828)
2-15	5305 (36 605)
3-15	5955 (41 090)
4-15	5747 (39 654)
5-15	5199 (35 873)
6-15	5269 (36 356)
7-15	5588 (38 557)

Average maximum compressive stress: 5589 psi (38 564 kN/m²)
Coefficient of variation: 6.19 percent

2.0 Percent Fiber

<u>Cylinder</u>	<u>Stress at Failure, psi (kN/m²)</u>
1-20	6030 (41 607)
2-20	5711 (39 406)
3-20	6030 (41 607)
4-20	6260 (43 194)
5-20	5404 (37 288)
6-20	6161 (42 511)
7-20	5641 (38 923)

Average maximum compressive stress: 5932 psi (40 931 kN/m²)
Coefficient of variation: 5.36 percent

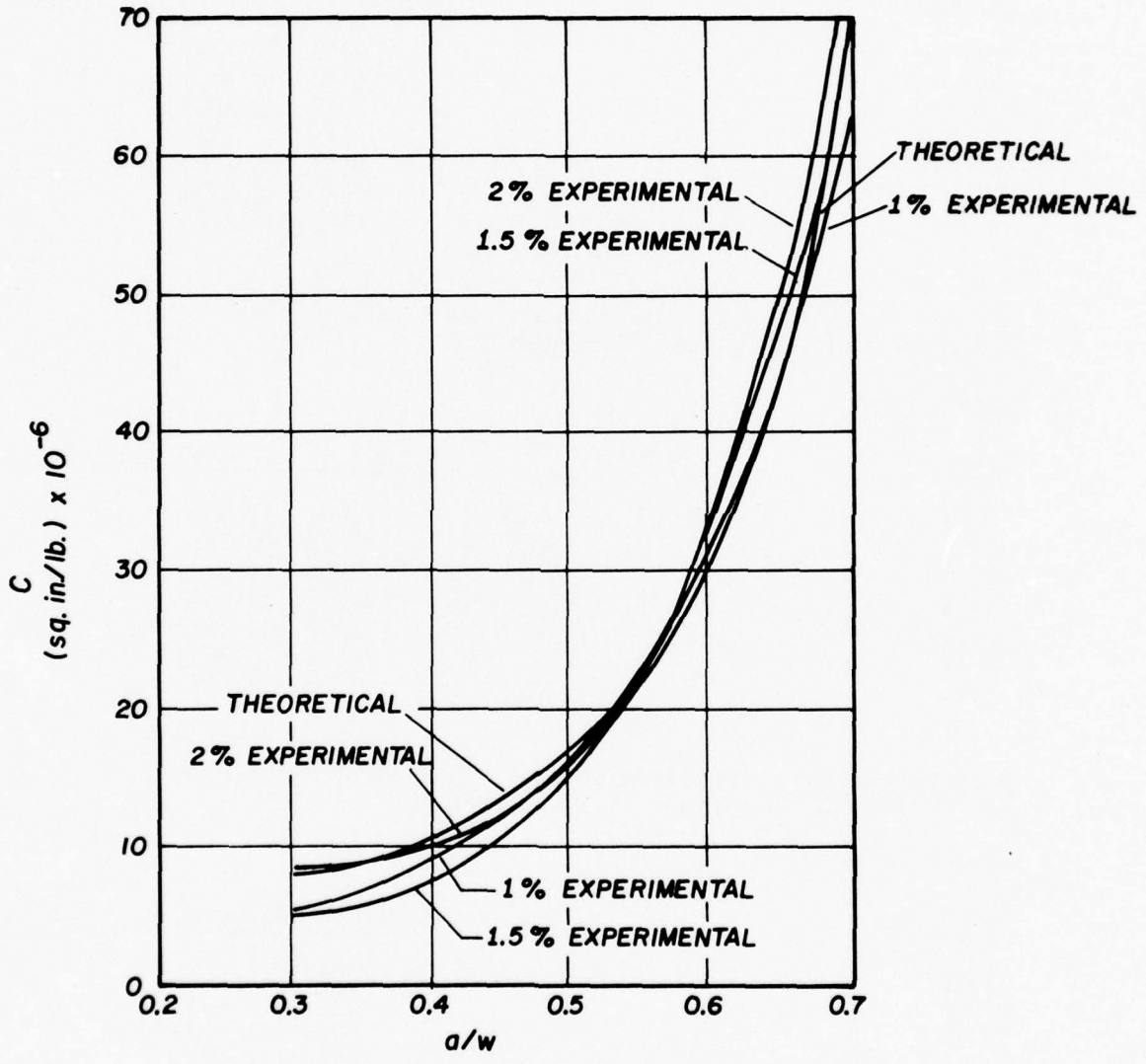


Figure 16. Theoretical compliance curve [Eq 6] and compliance curve fit for 1.0 [Eq 7], 1.5 [Eq 8], and 2.0 [Eq 9] percent fiber content. SI conversion factor: 1 sq in./lb = 0.14 m²/kN.

Table 7
Properties of Artificial
Saltwater Environment

Days	pH	Conductivity $\mu\text{mhos}/\text{cm}^2$	Salt Content %	Temperature $^{\circ}\text{F}$ ($^{\circ}\text{C}$)
0.0	7.20	54 350	4.00	70 (21)
0.2	8.80	52 990	unk.	70 (21)
1.0	8.80	52 990	unk	71 (22)
1.5	8.53	54 450	unk.	71 (22)
3.0	8.85	47 560	unk.	72 (22)
14	8.96	48 970	3.81	70 (21)
23	9.18	47 100	4.04	71 (22)
38	9.65	48 780	4.06	69 (21)
48	9.70	51 060	4.08	71 (22)
62	9.64	49 140	4.14	70 (21)
74	9.65	48 220	4.14	71 (22)
80	9.64	47 560	4.14	72 (22)
102	9.65	47 840	4.04	73 (23)
113	9.64	47 640	4.02	72 (22)
130	9.62	47 330	4.00	72 (22)
148	9.66	46 880	4.02	72 (22)
152*	7.30	48 930	3.91	76 (24)
161	8.80	48 530	4.06	72 (22)
176	8.83	47 800	4.04	71 (22)

*Occurrence of an accidental drainage required the replenishment of the entire environmental system. This accounts for the discrepancies in subsequent pH and temperature values.

4 DISCUSSION OF TEST RESULTS

The G_{IC} values for both the control and environmental specimens increased with increasing fiber contents. Thus, for any given exposure interval, it is expected that the concrete with the greater percentage of steel fibers will require a larger strain energy release rate for crack propagation.

A comparison of the 1.5 and 2.0 percent fiber content specimens showed that the 2.0 percent specimens required a 20 percent increase in the strain energy release rate for crack propagation. Figure 12 shows that increasing the percentage of steel fibers in the specimens increases the relative strength of the concrete for any given interval of exposure to the adverse environment. Thus, the higher the fiber concentration in the concrete, the less it is affected by exposure to the adverse environment.

The trend of all three curves in Figure 12 is toward a decreasing slope with increasing time of exposure. It would be both interesting and beneficial to carry out the experiment for a longer duration, 1 year for example, to determine whether the decreasing slope trend continues or whether the relative G_{IC} values asymptotically approach some minimum value. Significant benefits of an even longer test duration would be to determine whether the change in pH of the concrete had any effect on its resistance to the saltwater environment.

The control specimen testing program indicated that the change in fiber content had little effect on the compliance curves or their first derivatives. This was also true for the range of a/w ratios used throughout the environmental testing process. Thus, only one fiber content need be tested to determine a compliance curve. Also, the excellent agreement with the theoretical compliance relationship would probably eliminate the need for an experimentally determined curve. A reduction in the number of samples and hence the quantity of materials required, and the facilitation of the testing process itself would more than compensate for the slight reduction in accuracy.

It was found that no more than one compliance data point could be generated from each control specimen. The attempts to generate multiple data points from a single specimen produced extremely erratic and inconclusive results. The exact cause of this behavior in the control specimens is unknown. Other investigations using a centrally notched beam of plain mortar have been able to load and unload the specimens several times.^{25,26} A partial explanation may be that the first

²⁵J. H. Brown, "The Failure of Glass-Fiber-Reinforced Notched Beams in Flexure," *Magazine of Concrete Research*, Vol 25, No. 82 (March 1973), p 31.

²⁶J. H. Brown, "Measuring the Fracture Toughness of Cement Paste and Mortar," *Magazine of Concrete Research*, Vol 24, No. 81 (December 1972), p 185.

maximum loading causes significant amounts of debonding between fibers and mortar ahead of the crack, analogous to the plastic enclave developed at the tip of a crack in metal. If this were the case, then the methyl red dye probably would not penetrate and define the true length of the new crack. The shape of the load-deflection curve on the autographic recorder appeared normal; therefore, the difficulty was probably with determination of the crack length.

The increase in pH of the solution indicated that a reaction was taking place between the saltwater and the fibrous concrete. The pH increase was to be expected, since fresh concrete has a pH of approximately 10 to 12.²⁷ Additional indication of a reaction between the saltwater and the fibrous concrete was the corrosion of the steel fibers in the environmental specimens. With the exception of the specimens exposed for 74 days, all the environmental specimens showed visible evidence of corrosive action. The fibers exposed to the flowing saltwater by the mechanical cracking had rust and corrosion visible through a hand-held magnifying glass.

The lower fiber content control specimens did not have a significant region of stable crack growth for the lower a/w ratios. The values of P_Q for the 1.0 percent fiber and shallow notch depth for the control specimens exceeded 90 percent of the corresponding P_p values. By comparison, similar ratios with 1.5 and 2.0 percent fiber yielded values of 80 and 82 percent, respectively. The specimens with 1.0 percent fiber also appeared to encounter an upper limit for a/w, whereas the higher fiber content demonstrated no such limit throughout the range of notch ratios tested. The consistently low G_{IC} values obtained for the 1.0 percent fiber specimens with high notch depths ($a/w \geq 0.60$) were not observed for the specimens containing a greater percentage of steel fibers.

After 150 days of exposure, an accidental drainage depleted the entire environmental system. The system was replenished within 24 hours. It can be assumed that this drainage had a minimal effect on the outcome of the experiment because the G_{IC} values of the remaining specimens followed the trends established by the previously tested environmental specimens (Figure 12).

²⁷I. Biczok, *Concrete Corrosion and Concrete Protection* (Chemical Publishing Co., 1967), p 243.

5 POTENTIAL STRUCTURAL APPLICATIONS

Fracture mechanics allows the determination of a crack size, such as the length or depth of a crack, in a structural element that will grow or propagate for a given stress field. Alternatively, for a given size of crack, the stress to cause growth or propagation can be evaluated.

The experimentally determined values of G_{IC} in this study are related to the stress intensity factor K_I by Eq 10.

$$G_{IC} = \frac{K_I^2}{E} \quad [\text{Eq 10}]$$

The K_I equations for a wide variety of crack and stress field configurations are available in the technical literature and handbooks.²⁸

As an example, consider a crack of depth a in a beam or slab of total depth b subjected to a pure bending moment as shown in Figure 17.

Assume

$$\begin{aligned} a &= 1 \text{ in. (25.4 mm)} \\ b &= 4 \text{ in. (101.6 mm)} \\ E &= 3 \times 10^6 \text{ psi (20.7} \times 10^6 \text{ kN/m}^2) \\ G_{IC} &= 0.85 \text{ (in.-lb)/sq in. (148.9 m-N/m}^2) \text{ ambient (lab) conditions} \\ G_{IC} &= 0.79 \text{ (in.-lb)/sq in. (138.4 m-N/m}^2) \text{ 176 days exposure to} \\ &\text{flowing saltwater} \end{aligned}$$

Tada, Paris, and Irwin give K_I in the opening mode as

$$K_I = \sigma \sqrt{\pi a} F(a/b) \quad [\text{Eq 11}]$$

where σ = maximum flexure stress

a = depth of crack

b = total depth of beam or slab

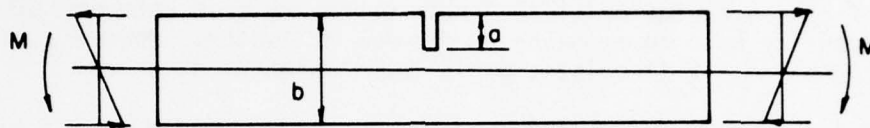
$F(a/b)$ = correction for finite boundary.

From Tada, Paris, and Irwin,

$$F(a/b) = 1.05$$

Therefore $\sigma = 901 \text{ psi (6217 kN/m}^2) \text{ ambient (lab) conditions}$
 $\sigma = 827 \text{ psi (5706 kN/m}^2) \text{ saltwater exposure.}$

²⁸H. Tada, P. Paris, and G. Irwin, *The Stress Analysis of Cracks Handbook* (Del Research Corporation, 1973).



$$G_{Ic} = \frac{K_I^2}{E} = \frac{\sigma^2 \pi a [CF(\frac{a}{b})]^2}{E}$$

Figure 17. Strength analysis of crack member in bending.

Using the G_{Ic} values 0.85 for ambient laboratory conditions and 0.79 for the saltwater exposure as determined from the data in this report, an estimate of the maximum flexure stress can be made for given crack size a , slab depth b , and Young's Modulus of the concrete. An a of 1 in. (25.4 mm), b of 4 in. (101.6 mm), and E of 3×10^6 psi (20.7×10^6 kJ/m²) give flexural stress of 901 psi (6217 kN/m²) for ambient conditions and 827 psi (5706 kN/m²) for saltwater exposure. The flexural stress will probably be somewhat lower since the test data indicate that the G_{Ic} was continuing to decrease relative to time. However, the values for the flexural stress are reasonable when compared to flexural stresses of 1000 to 1200 psi (6900 to 8280 kN/m²) for beams tested in flexure.

The load-carrying capacity of a cracked steel-fiber-reinforced concrete structural element (such as a slab or beam) subject to saltwater is reduced, but the calculations show that there is still significant flexural strength remaining at reduced loads. Thus, the strength can be estimated; this estimate can be used to decide whether to continue to use the structure at a reduced load, repair it, or replace it.

6 CONCLUSIONS AND RECOMMENDATIONS

For the three fiber contents of 1.0, 1.5, and 2.0 percent by volume of concrete, the critical strain energy release rate decreased at a decreasing rate in exposure to flowing saltwater. However, an asymptotic value, if it exists, would require longer exposure.

The 2.0 percent fiber content specimens were least affected by the adverse environment. After 176 days of exposure, the G_{IC} value for these specimens was 89 percent of the average ambient value, while values for 1.5 and 1.0 percent fiber content specimens were 81 and 66 percent, respectively.

The increase in pH of saltwater solution indicated a reaction between the saltwater and the concrete matrix, while evidence of rust on the fibers indicated a reaction between the flowing saltwater and the steel fibers.

Increasing the steel fiber concentration did not significantly alter the compliance values of the modified WOL specimens for the three fiber contents investigated. Furthermore, the first derivatives of the experimental compliance curves for the fiber contents involved demonstrated excellent correlation with the theoretical values obtained from collocation of a stress function.

The G_{IC} values determined in this report can be used to estimate the flexural strength of steel-fiber-reinforced concrete structural elements.

The results of this study indicate the need for the following additional research:

1. Increase the total duration of exposure to 3 years to determine whether the strength of the fibrous concrete asymptotically approaches some lower limit. The longer test would also help determine the effects of the adverse environment on the natural pH change of the concrete.
2. Alter the corrosive environment by adding a buffer to the saltwater solution; doing so would tend to maintain the pH of the solution at a lower level.
3. Perform the entire experiment with only one fiber content, but with a sufficient number of environmental specimens to develop a compliance relationship among those specimens exposed to the saltwater.
4. Use smaller size specimens to further reduce the size of the environmental tank and facilitate the handling of specimens.
5. Test the effect of the adverse environment on concrete of different strengths to determine if the deleterious effect of the flowing saltwater is a function of the strength of the concrete.

APPENDIX A:
FRACTURE MECHANICS THEORY

Fracture mechanics concepts for explaining the failure of brittle materials were pioneered in 1921 by A. A. Griffith,²⁹ who showed that a material failure could be described by relating the existence of minute flaws in a material to an energy condition necessary for crack propagation. Considering W as the reduction in stored elastic energy due to the presence of a crack in a fixed grip system, and U as the energy of the crack surface, a crack of radius a will propagate if

$$\frac{\partial (W-U)}{\partial a} = 0 \quad [\text{Eq A1}]$$

Simply stated, a crack will propagate in a material if the elastic energy release rate is equal to the irrecoverable work required to create an area of crack surface.

Applying Eq A1 to a homogeneous plate of unit thickness subjected to a tensile stress field σ and containing a central through the thickness crack of length $2a$ perpendicular to the stress field³⁰ gives

$$W = \frac{\pi\sigma^2 a^2}{E} \quad [\text{Eq A2}]$$

and
$$U = 4Ta \quad [\text{Eq A3}]$$

where T = the specific surface energy of the crack

E = the modulus of elasticity.

For a crack to propagate, the following condition must apply:

$$\frac{\partial}{\partial a} \left(\frac{\pi\sigma^2 a^2}{E} \right) - 4T = 0 \quad [\text{Eq A4a}]$$

or

$$\frac{2\pi\sigma^2 a}{E} = 4T \quad [\text{Eq A4b}]$$

Eq A4b can be solved for the applied tensile stress necessary for crack propagation:

$$\sigma = \left(\frac{2TE}{\pi a} \right)^{1/2} \quad [\text{Eq A5}]$$

²⁹A. A. Griffith, "Phenomena of Rupture and Flow in Solids," *Philosophical Transactions*, Vol 221, No. A587 (Royal Society of London, 1921), p 163.

³⁰J. P. Romualdi and G. B. Batson, "Mechanics of Crack Arrest in Concrete," *Journal of the Engineering Mechanics Division, Proceedings of the American Society of Civil Engineers*, Vol 89, No. EM3 (June 1963), p 147.

It has been an accepted procedure in fracture mechanics to denote the left side of Eq A4b by G , the elastic energy release rate, and the right side by G_c , the work rate to extend the crack. G is a function of the geometry of the specimen and the loading, while G_c is a material constant.³¹ A crack will propagate in a material provided that

$$G \geq G_c = 4T \quad [\text{Eq A6}]$$

If, however, G is less than the critical value, G_c , crack propagation will not occur.

In 1960, G. R. Irwin³² related the G value to another parameter, which he termed the stress intensity factor, K , in the following manner:

$$G = \frac{K^2}{E} \quad (\text{for plane stress}) \quad [\text{Eq A7a}]$$

$$G = \frac{K^2}{E} (1-\nu^2) \quad (\text{for plane strain}) \quad [\text{Eq A7b}]$$

where ν = Poisson's ratio.

The stress intensity factor, K , relates the stress in the vicinity of the crack tip to the geometry of a crack or flaw, usually the length or radius of the flaw.

The stress intensity factor has great value in fracture mechanics analysis because the total stress intensity factor can be determined by the superposition of the K values for each individual stress field.

In summary, the minute flaws of many brittle materials, when subjected to a stress field of sufficient magnitude, become the locus of a crack propagating through the material. This situation can be remedied by reducing the dimensions of the inherent material flaws or by inhibiting their growth by physical means. The physical inhibitors used in this study were discrete steel fibers added directly to the concrete mix.

³¹Romualdi and Batson, p 147.

³²G. R. Irwin and J. A. Kies, "Critical Energy Rate Analysis of Fracture Strength," *Welding Journal*, Vol 33 (April 1954), p 193s.

APPENDIX B:
CURVE FIT DERIVATION AND COMPUTER PROGRAM

Curve Fit Derivation

Fitting a curve through a set of data subject to the condition that the first derivative of the equation of the curve is zero at the point (0,0) involves elimination of the linear term from the equation of the curve.

Consider C_1 through C_m to be m values of a dependent variable corresponding to m values of an independent variable x . A curve of the n th order in x is to be fit through these points by a polynomial least square curve fit. Letting a_0 through a_n be the coefficients of the n th order curve gives

$$\begin{array}{r}
 a_0 + a_2x_1^2 + a_3x_1^3 + \dots + a_nx_1^n = C_1 \\
 a_0 + a_2x_2^2 + a_3x_2^3 + \dots + a_nx_2^n = C_2 \\
 \cdot \quad \cdot \quad \cdot \quad \cdot \quad \cdot \\
 \cdot \quad \cdot \quad \cdot \quad \cdot \quad \cdot \\
 \cdot \quad \cdot \quad \cdot \quad \cdot \quad \cdot \\
 a_0 + a_2x_m^2 + a_3x_m^3 + \dots + a_nx_m^n = C_m
 \end{array}
 \quad [Eq B1]$$

The absence of an a_1x term from the equations insures the lack of a linear term in the resulting curve.

Expressing the above equations in matrix form results in the following:

$$\begin{bmatrix}
 1 & x_1^2 & x_1^3 & \dots & x_1^n \\
 1 & x_2^2 & x_2^3 & \dots & x_2^n \\
 \cdot & \cdot & \cdot & \cdot & \cdot \\
 \cdot & \cdot & \cdot & \cdot & \cdot \\
 \cdot & \cdot & \cdot & \cdot & \cdot \\
 1 & x_m^2 & x_m^3 & \dots & x_m^n
 \end{bmatrix}
 \begin{bmatrix}
 a_0 \\
 a_2 \\
 a_3 \\
 \cdot \\
 \cdot \\
 a_n
 \end{bmatrix}
 =
 \begin{bmatrix}
 C_1 \\
 C_2 \\
 C_3 \\
 \cdot \\
 \cdot \\
 C_m
 \end{bmatrix}
 \quad [Eq B2]$$

or

$$XA = C \quad [Eq B3]$$

where X is of order $m \times n$ (not necessarily square), A is of order $n \times 1$, and C is of order $m \times 1$.

Inverting the X matrix will generally not be possible. This does not, however, preclude obtaining the coefficient matrix, A , after a few basic matrix manipulations. First, both sides of the equation are premultiplied by the transpose of the X matrix, giving

$$X^T X A = X^T C \quad [\text{Eq B4}]$$

The $X^T C$ matrix (designated \bar{C}) is of order $n \times 1$, and $X^T X$ (designated \bar{X}) is of order $n \times n$ and invertible. Solving for the coefficient matrix A gives

$$\bar{X} A = \bar{C} \quad [\text{Eq B5}]$$

$$(\bar{X})^{-1} \bar{X} A = (\bar{X})^{-1} \bar{C} \quad [\text{Eq B6}]$$

$$A = (\bar{X})^{-1} \bar{C} \quad [\text{Eq B7}]$$

The resulting A matrix will be the polynomial least square coefficients for a curve of the n^{th} order with first power term eliminated and the coefficients arranged in order of increasing powers of the independent variables.

Curve Fit Program

The following program, written by John K. Obzsarski of Clarkson College of Technology, is designed to provide a polynomial least square curve fit of the input data. The program was designed for the IBM 380 digital computer model 44 at Clarkson College of Technology in Potsdam, NY.

The program is capable of fitting a curve of up to tenth order through no more than 30 pieces of data. If there are more than 30 data points, or if a curve fit of greater than tenth order is desired, alteration of the dimension statements in the main program will be the only changes necessary.

The program will fit a curve from second order to the maximum order specified in the input data. A table of residuals and error analysis is printed for each order polynomial.

The program has been designed so that the linear term of each polynomial has been forced to zero, thus providing a zero slope at the point (0.0).

The input data must be arranged in the following order:

Card 1:

Columns 1-4 The number of data points to be evaluated (integer).

Columns 5-8 The highest order polynomial (up to tenth) for which a curve fit is desired (integer).

Columns 9-15 The fiber content of the specimens evaluated (real).

Card 2:

Columns 1-20 The type of specimen involved (alpha-numeric)

The remainder of the cards contain the data points through which a curve is to be fit.

Columns 1-10 The independent variable, a/w (real)

Columns 11-20 The dependent variable, compliance (real)

All integer inputs must be right-justified.

The subroutines internal to this program, which are contained in the printout on pages 46 to 52, are a data sorting and arranging routine called SORT. The polynomial least square curve fitting routine--POLSC, and a matrix inversion routine called MINV.

There are no subroutines external to this program.

```

DIMENSION CLSQ(30),DIFF(30),COINC(31),COEFF(10)
DIMENSION JJ(60)
DIMENSION TYPE(E)
INTEGER POLYC, CRDR,OP1
COMMON D,DT
1 FORMAT(2I4,F6.2)
2 FORMAT(2F10.4)
3 FORMAT('1')
4 FORMAT(5A4)
5 FORMAT(' POLYNOMIAL LEAST SQUARE CURVE FIT:',F6.2,' PERCENT FIBER.
1',18X,'TYPE OF SPECIMEN: ',5A4//)
6 FORMAT(' ANALYSIS FOR POLYNOMIAL OF ORDER',I3,' FOLLOWS://///')
7 FORMAT(' NUMBER OF OBSERVATIONS:',I4//)
8 FORMAT(' NOTE: THE COEFFICIENT OF THE FIRST POWER TERM HAS BEEN'/
1' FORCED TO ZERO IN ORDER TO PROVIDE A FIRST DERIVATIVE OF 0.0'/
2,' AT THE POINT (0,0).')//)
9 FORMAT(' THE FOLLOWING COEFFICIENTS ARE ARRANGED IN ORDER'/
1,' OF INCREASING POWERS OF THE INDEPENDENT VARIABLE.//)
10 FORMAT(' ',F10.4)
11 FORMAT('0',33X,' TABLE OF RESIDUALS'/////
1,5X,' OBSERVATION', 7X,'A/W',11X,'COMPLIANCE',10X,'COMPLIANCE',12X
2,'RESIDUAL'/
3,40X,'ACTUAL',13X,'CURVE FIT'//)
12 FORMAT(I12,F16.3,F19.2,F20.2,F20.2)
13 FORMAT('0',' THE SUM OF THE SQUARE OF THE RESIDUALS IS',F10.4/
1,' THE NUMBER OF DEGREES OF FREEDOM OF THE POLYNOMIAL IS',I3)
14 FORMAT('0',' THE DEGREE OF FREEDOM OF THE CURVE IS ZERO.'/
1,' A HIGHER ORDER CURVE CANNOT BE FIT THROUGH'/
2,' THE EXISTING DATA.')
```

C
C
C

```

1000 CONTINUE
READ(1,1,END=999)NDP,POLYC,PFBR
READ(1,4)(TYPE(I),I=1,5)
DO 20 I=1,NDP
READ(1,2) AW(I), COMP(I)
20 CONTINUE
```

C
C
C
C
C
C
C

```

THE DATA ARE SORTED BY MAGNITUDE
OF THE INDEPENDENT VARIABLE, HIGHEST BEING FIRST.

CALL SORT(NDP,AW,COMP)

A CURVE FIT OF THE DATA
IS NOW INITIATED. CURVES ARE FIT
FROM SECOND ORDER TO THE HIGHEST
ORDER SPECIFIED IN THE DATA INPUT .

DO 30 ORDER=2,POLYC
NCOF=NDP-ORDER-1
DOF=NCOF
```

```

        IF(DOF)210,65,65
65    CONTINUE
        NP21=ORDER+21
C
C    A POLYNOMIAL LEAST SQUARE FIT OF THE DATA
C    IS ACCOMPLISHED BY MEANS OF THE FOLLOWING
C    SUBROUTINE.
C
C    CALL POLSQ(AW,COMP,ORDER,NDP,COEFF,CLSQ,AWP,AWC,AWS,JJ,NP21)
C
C    AFTER A POLYNOMIAL HAS BEEN FIT
C    TO THE DATA, THE ERROR OF ESTIMATE IS COMPUTED.
C
        SUMSQ=0.
        DO 140 I=1,NDP
        DIFF(I)=COMP(I)-CLSQ(I)
140    SUMSQ=SUMSQ+(DIFF(I)**2)
        WRITE(3,3)
        WRITE(3,5)PFBR,(TYPE(I),I=1,5)
        WRITE(3,6)ORDER
C
C    IF THE DETERMINATE OF THE
C    INVERTED MATRIX IS ZERO, ALL VALUES
C    ARE REJECTED AS ERRONEOUS.
C
        IF(D) 130,220,130
220    CONTINUE
        WRITE(3,17)
        WRITE(3,18)
        WRITE(3,17)
        ORDER=POLYO
        GO TO 30
130    CONTINUE
        WRITE(3,7)NDP
        COINC(1)=COEFF(1)
        CCINC(2)=0.0
        DO 150 I=2,ORDER
        IP1=I+1
150    CCINC(IP1)=CCEFF(I)
        WRITE(3,8)
        OP1=ORDER+1
        WRITE(3,9)
        WRITE(3,10)(COINC(I),I=1,OP1)
        WRITE(3,11)
        DO 160 I=1,NDP
160    WRITE(3,12)I,AW(I),COMP(I),CLSQ(I),DIFF(I)
        IF(DOF.EQ.0.0) GC TO 200
        GROSE=SUMSQ/DOF
        WRITE(3,13)SUMSG,NDOF
        WRITE(3,16)GRCSE
        GO TO 30
200    WRITE(3,14)
        WRITE(3,13)SUMSG,NDOF
        ORDER=POLYO
        GO TO 30
210    WRITE(3,15)
        ORDER=PCLYO
        30    CONTINUE
        GO TO 1000
599    STOP

```

```

END
SUBROUTINE POLSQ(AW,COMP,NRDER,NDP,COEFF,CLSQ,AWP,AWC,AWS,JJ,NP21)
DIMENSION AWP(NCP,NRDER),AWC(NRDER),AWS(NRDER,NRDER)
DIMENSION CLSQ(NDP),AW(NDP),COMP(NDP),COEFF(NRDER)
DIMENSION JJ(NP21)
INTEGER ORDER
COMMON D,DT
ORDER=NRDER
N=ORDER
DO 40 I=1,NDP
40 AWP(I,1)=1.
DO 50 I=1,NDP
50 AWP(I,N)=(AW(I))*N
DO 70 I=1,ORDER
DO 70 J=1,ORDER
70 AWS(I,J)=0.
DO 80 I=1,ORDER
DO 80 J=1,ORDER
DO 80 K=1,NDP
80 AWS(I,J)=AWS(I,J)+(AWP(K,J)*AWP(K,I))
DO 100 I=1,ORDER
AWC(I)=0.
DO 100 J=1,NDP
100 AWC(I)=AWC(I)+(COMP(J)*AWP(J,I))
CALL MINV(AWS,NRDER,NP21,DT,D,JJ)
DO 110 I=1,ORDER
CCEFF(I)=0.
DO 110 J=1,ORDER
110 COEFF(I)=COEFF(I)+(AWS(I,J)*AWC(J))
DO 130 I=1,NDP
CLSQ(I)=0.
DO 130 J=1,ORDER
130 CLSQ(I)=CLSQ(I)+(AWP(I,J)*COEFF(J))
RETURN
END
SUBROUTINE SORT(NDP,AW,COMP)
DIMENSION AW(NDP),COMP(NDP)
NDPM1=NDP-1
DO 30 I=1,NDPM1
IP1=I+1
DO 30 J=IP1,NDP
IF(AW(I).GE.AW(J)) GO TO 30
R=AW(J)
R1=COMP(J)
AW(J)=AW(I)
COMP(J)=COMP(I)
AW(I)=R
COMP(I)=R1
30 CONTINUE
RETURN
END
SUBROUTINE MINV(C,N,NEXP,DTNRM,DETM,JJ)
DIMENSION C(N,N),JJ(NEXP)
PD=1.
DO 124 L=1,N
DD=0.
DO 123 K=1,N
123 DD=DD+C(L,K)*C(L,K)
DD=DD**.5
124 PD=PD*DD

```

```

      DETM=1.
      DC 125 L=1,N
125  JJ(L+20)=L
      DO 144 L=1,N
      CC=0.
      M=L
      DO 135 K=L,N
      IF((ABS(CC)-ABS(C(L,K))).GE.0.) GO TO 135
126  M=K
      CC=C(L,K)
135  CONTINUE
127  IF(L.EQ.M) GO TO 138
128  K=JJ(M+20)
      JJ(M+20)=JJ(L+20)
      JJ(L+20)=K
      DO 137 K=1,N
      S=C(K,L)
      C(K,L)=C(K,M)
137  C(K,M)=S
138  C(L,L)=1.
      DETM=DETM*CC
      DO 139 M=1,N
139  C(L,M)=C(L,M)/CC
      DO 142 M=1,N
      IF(L.EQ.M) GO TO 142
129  CC=C(M,L)
      IF(CC.EQ.0.) GO TO 142
130  C(M,L)=0.
      DO 141 K=1,N
141  C(M,K)=C(M,K)-CC*C(L,K)
142  CONTINUE
144  CONTINUE
      DC 143 L=1,N
      IF(JJ(L+20).EQ.L) GO TO 143
131  M=L
132  M=M+1
      IF(JJ(M+20).EQ.L) GO TO 133
136  IF (N.GT.M) GO TO 132
133  JJ(M+20)=JJ(L+20)
      DC 163 K=1,N
      CC=C(L,K)
      C(L,K)=C(M,K)
163  C(M,K)=CC
      JJ(L+20)=L
143  CONTINUE
      DETM=ABS(DETM)
      DTNRM=DETM/PC
      RETURN
      END

```

POLYNOMIAL LEAST SQUARE CURVE FIT: 1.00 PERCENT FIBER.
TYPE OF SPECIMEN: COMPLIANCE

ANALYSIS FOR POLYNOMIAL OF ORDER 4 FOLLOWS:

NUMBER OF OBSERVATIONS: 17

NOTE: THE COEFFICIENT OF THE FIRST POWER TERM HAS BEEN FORCED TO ZERO IN ORDER TO PROVIDE A FIRST DERIVATIVE OF 0.0 AT THE POINT (0,0).

THE FOLLOWING COEFFICIENTS ARE ARRANGED IN ORDER OF INCREASING POWERS OF THE INDEPENDENT VARIABLE

0.2441
0.0
144.6875
-492.1875
663.6875

TABLE OF RESIDUALS

OBSERVATION	A/W	COMPLIANCE ACTUAL	COMPLIANCE CURVE FIT	RESIDUAL
1	0.680	58.68	54.29	4.39
2	0.672	47.83	51.57	-3.74
3	0.664	49.20	48.96	0.24
4	0.640	39.27	41.83	-2.56
5	0.563	30.61	24.95	5.66
6	0.555	24.28	23.64	0.64
7	0.547	20.50	22.40	-1.90
8	0.523	16.58	19.07	-2.49
9	0.422	9.73	10.07	-0.34
10	0.410	9.67	9.40	0.27
11	0.398	8.97	8.79	0.18
12	0.398	10.13	8.79	1.34
13	0.390	8.44	8.41	0.03
14	0.387	7.18	8.27	-1.10
15	0.360	7.53	7.18	0.35
16	0.330	5.64	6.18	-0.54
17	0.0	0.33	0.24	0.09

THE SUM OF THE SQUARE OF THE RESIDUALS IS 85.6738
THE NUMBER OF DEGREES OF FREEDOM OF THE POLYNOMIAL IS 12
THE GROSS ERROR OF ESTIMATE IS 7.1395

POLYNOMIAL LEAST SQUARE CURVE FIT: 1.50 PERCENT FIBER.
TYPE OF SPECIMEN: COMPLIANCE

ANALYSIS FOR POLYNOMIAL OF ORDER 4 FOLLOWS:

NUMBER OF OBSERVATIONS: 15

NOTE: THE COEFFICIENT OF THE FIRST POWER TERM HAS BEEN FORCED TO ZERO IN ORDER TO PROVIDE A FIRST DERIVATIVE OF 0.0 AT THE POINT (0,0).

THE FOLLOWING COEFFICIENTS ARE ARRANGED IN ORDER OF INCREASING POWERS OF THE INDEPENDENT VARIABLE

0.6975
0.0
162.3125
-644.7500
871.7500

TABLE OF RESIDUALS

OBSERVATION	A/W	COMPLIANCE ACTUAL	COMPLIANCE CURVE FIT	RESIDUAL
1	0.688	59.90	62.88	-2.98
2	0.656	56.60	49.97	6.63
3	0.656	48.14	49.97	-1.83
4	0.531	18.13	19.24	-1.11
5	0.523	18.62	18.08	0.54
6	0.521	17.39	17.81	-0.42
7	0.521	17.47	17.81	-0.34
8	0.450	9.90	10.56	-0.66
9	0.438	8.69	9.74	-1.06
10	0.435	9.28	9.55	-0.27
11	0.398	8.50	7.63	0.87
12	0.380	6.96	6.93	0.03
13	0.380	8.00	6.93	1.07
14	0.281	5.27	4.64	0.63
15	0.0	0.33	0.70	-0.36

THE SUM OF THE SQUARE OF THE RESIDUALS IS 61.9932
THE NUMBER OF DEGREES OF FREEDOM OF THE POLYNOMIAL IS 10
THE GROSS ERROR OF ESTIMATE IS 6.1993

POLYNOMIAL LEAST SQUARE CURVE FIT: 2.00 PERCENT FIBER.
TYPE OF SPECIMEN: COMPLIANCE

ANALYSIS FOR POLYNOMIAL OF ORDER 4 FOLLOWS:

NUMBER OF OBSERVATIONS: 15

NOTE: THE COEFFICIENT OF THE FIRST POWER TERM HAS BEEN FORCED TO ZERO IN ORDER TO PROVIDE A FIRST DERIVATIVE OF 0.0 AT THE POINT (0,0).

THE FOLLOWING COEFFICIENTS ARE ARRANGED IN ORDER OF INCREASING POWERS OF THE INDEPENDENT VARIABLE

0.0349
0.0
391.7500
-1480.3125
1634.8125

TABLE OF RESIDUALS

OBSERVATION	A/W	COMPLIANCE ACTUAL	COMPLIANCE CURVE FIT	RESIDUAL
1	0.680	63.31	65.27	-1.96
2	0.672	62.32	61.11	1.21
3	0.656	55.10	53.48	1.62
4	0.551	22.08	22.02	0.06
5	0.531	17.01	18.83	-1.82
6	0.516	18.13	16.86	1.27
7	0.516	14.97	16.86	-1.89
8	0.512	16.14	16.39	-0.25
9	0.422	13.12	10.40	2.72
10	0.406	11.19	9.96	1.23
11	0.406	10.29	9.96	0.33
12	0.391	8.50	9.65	-1.14
13	0.387	10.05	9.58	0.47
14	0.313	6.74	8.71	-1.97
15	0.0	0.33	0.03	0.30

THE SUM OF THE SQUARE OF THE RESIDUALS IS 31.0459
THE NUMBER OF DEGREES OF FREEDOM OF THE POLYNOMIAL IS 10
THE GROSS ERROR OF ESTIMATE IS 3.1046

CITED REFERENCES

- Annual Book of ASTM Standards* (American Society for Testing and Materials, May 1969), Part 31.
- Batson, G. B. et al., "Flexural Fatigue of Steel Fiber Reinforced Concrete Beams," *Journal of the American Concrete Institute*, Proceedings Vol 69, No. 11 (November 1972), p 673.
- Batson, G. B., E. Jenkins, and R. Spatney, "Steel Fibers as Shear Reinforcement in Beams," *Journal of the American Concrete Institute*, Proceedings Vol 69, No. 10 (October 1972), p 640.
- Biczok, I., *Concrete Corrosion and Concrete Protection* (Chemical Publishing Co., 1967), p 243.
- Brown, J. H., "The Failure of Glass-Fiber-Reinforced Notched Beams in Flexure," *Magazine of Concrete Research*, Vol 25, No. 82 (March 1973), p 31.
- Brown, J. H., "Measuring the Fracture Toughness of Cement Paste and Mortar," *Magazine of Concrete Research*, Vol 24, No. 81 (December 1972), p 185.
- Desai, J. D. and W. W. Gerberich, "Analysis of Incremental Cracking by the Stress Wave Emission Technique," *Engineering Fracture Mechanics*, Vol 7 (Pergamon Press, 1975), p 156.
- Forzani, A. A., *Environmental Effects on Fiber Reinforced Concrete*, Unpublished M.S. Thesis (Clarkson College of Technology, 1972).
- Griffith, A. A., "Phenomena of Rupture and Flow in Solids," *Philosophical Transactions*, Vol 221, No. A587 (Royal Society of London, 1921), p 163.
- Gross, B., J. E. Srawley, and W. P. Brown, *Stress Intensity Factors for a Single Edge Notch Tension Specimen by Boundary Collocation of a Stress Function*, NASA Technical Note D 2395 (National Aeronautics and Space Administration [NASA], August 1964).
- Irwin, G. R. and J. A. Kies, "Critical Energy Rate Analysis of Fracture Strength," *Welding Journal*, Vol 33 (April 1954), p 193s.
- Knott, J. F., *Fundamentals of Fracture Mechanics* (Butterworths, 1973), p 105.
- Mathis, M. J., *Fracture Testing of Fiber Reinforced Concrete by Means of the Wedge Opening Loading Specimen*, Unpublished M.S. Thesis (Clarkson College of Technology, 1974).

- Romualdi, J. P. and G. B. Batson, "Mechanics of Crack Arrest in Concrete," *Journal of the Engineering Mechanics Division, Proceedings of the American Society of Civil Engineers*, Vol 89, No. EM3 (June 1963), p 147.
- Romualdi, J. P. and J. A. Mandel, "Tensile Strength of Concrete Affected by Uniformly Distributed and Closely Spaced Short Lengths of Wire Reinforcement," *Journal of the American Concrete Institute*, Proceedings Vol 61, No. 6 (June 1964), p 657.
- Srawley, J. E., M. H. Jones, and B. Gross, *Experimental Determination of the Dependence of Crack Extension Force on Crack Length for a Single Edge Notch Tension Specimen*, NASA Technical Note D 2396 (NASA, August 1964).
- Swamy, R. N. and P. S. Mangat, "The Onset of Cracking and Ductility of Steel Fiber Reinforced Concrete," *Cement and Concrete Research*, Vol 5 (1975), p 37.
- Symposium on Fracture Toughness Testing and Its Applications*, ASTM Special Technical Publication No. 381 (ASTM in cooperation with NASA, 1965).
- Tada, H., P. Paris, and G. Irwin, *The Stress Analysis of Cracks Handbook* (Del Research Corporation, 1973).
- Turner, C. E., "Fracture Toughness and Specific Fracture Energy: A Re-Analysis of Results," *Materials Science and Engineering*, Vol 11 (May 1973), pp 275-282.
- Wessel, E. T., "State of the Art of the WOL Specimen for K_{Ic} Fracture Toughness Testing," *Engineering Fracture Mechanics*, Vol 1 (1968), p 77.
- Woods, H., *Durability of Concrete Construction*, ACI Monograph #4 (American Concrete Institute, Iowa State University Press, 1968), p 137.

UNCITED REFERENCES

- Fisher, D. M., R. T. Bubsey, and J. E. Srawley, *Design of Use of Displacement Gage for Crack-Extension Measurements*, NASA Technical Note D 3724 (NASA, November 1966).
- Gross, B. T. and J. E. Srawley, *Stress Intensity Factors by Boundary Collocation for Single Edge Notch Specimens Subject to Splitting Forces*, NASA Technical Note D 3295 (NASA, February 1966).
- Gross, B. T. and J. E. Srawley, *Stress Intensity Factors for Three Point Bend Specimens by Boundary Collocation*, NASA Technical Note D 3092 (NASA, December 1965).

Hornbeck, R. W., *Numerical Methods* (Quantum Publishers, Inc., 1975),
p 295.

Ketter, R. L. and S. P. Prawel, *Modern Methods of Engineering Computa-
tion* (McGraw-Hill, 1969).

Neville, A. M. and J. B. Kennedy, *Basic Statistical Methods for Engineers
and Scientists* (International Textbook Company, 1964).

CERL DISTRIBUTION

Chief of Engineers
ATTN: DAEN-MCE-D
ATTN: DAEN-CWE-DC
ATTN: DAEN-CWE-DS
Department of the Army
WASH DC 20314

Defense Documentation Center
ATTN: TCA (12)
Cameron Station
Alexandria, VA 22314